Organic Spin Clusters. A Dendritic-Macrocyclic Poly(arylmethyl) Polyradical with Very High Spin of $S = 10$ and Its Derivatives: Synthesis, Magnetic Studies, and Small-Angle Neutron Scattering

Suchada Rajca,*,† Andrzej Rajca,*,† Jirawat Wongsriratanakul,† Paul Butler,‡ and Sung-min Choi§

Contribution from the Department of Chemistry, University of Nebraska, Lincoln, Nebraska 68588-0304, and The National Center for Neutron Research, NIST, Gaithersburg, Maryland 20899-8562

Received December 5, 2003; E-mail: srajca1@unl.edu; arajca1@unl.edu

Abstract: Synthesis and characterization of organic spin clusters, high-spin poly(arylmethyl) polyradicals with 24 and 8 triarylmethyls, are described. Polyether precursors to the polyradicals are prepared via modular, multistep syntheses, culminating in Negishi cross-couplings between four monofunctional branch (dendritic) modules and the tetrafunctional calix[4]arene-based macrocyclic core. The corresponding carbopolyanions are prepared and oxidized to polyradicals in tetrahydrofuran-d_8. The measured values of S, from numerical fits of magnetization vs magnetic field data to Brillouin functions at low temperatures ($T = 1.8–5$ K), are $S = 10$ and $S = 3.6–3.8$ for polyradicals with 24 and 8 triarylmethyls, respectively. Magnetizations at saturation (M_{sat}) indicate that 60–80% of unpaired electrons are present at $T = 1.8–5$ K. Low-resolution shape reconstructions from the small-angle neutron scattering (SANS) data indicate that both the polyradical with 24 triarylmethyls and its derivatives have dumbbell-like shapes with overall dimensions $2 \times 3 \times 4$ nm, in agreement with the molecular shapes of the lowest energy conformations obtained from Monte Carlo conformational searches. On the basis of these shapes, the size of the magnetic anisotropy barrier in the polyradical, originating in magnetic shape anisotropy, is estimated to be in the milliKelvin range, consistent with the observed paramagnetic behavior at $T \geq 1.8$ K. For macromolecular polyradicals, with the elongated shape and the spin density similar to the polyradical with 24 triarylmethyls, it is predicted that the values of S on the order of 1000 or higher may be required for "single-molecule-magnet" behavior, i.e., superparamagnetic blocking (via coherent rotation of magnetization) at the readily accessible temperatures $T > 2$ K.

Introduction

Molecules with large values of quantum spin number S in the electronic ground states may be viewed as models for organic polymers with magnetic ordering.[1–4] Design and synthesis of such molecules (polyradicals) must ensure that strong through-bond exchange interactions between multiple sites with unpaired electrons (radicals) are maintained.[4] Even if very efficient synthetic methods for generation of radicals are employed, the finite probability that generation of radicals will not be complete must be taken into account, i.e., formation of chemical defects. Therefore, connectivity between radicals should be such that strong exchange interaction between the radicals is sustained in the presence of small density of chemical defects.[5–7] Furthermore, out-of-plane twistings of the conjugated system may lead to the ferromagnetic-to-antiferromagnetic coupling reversals, diminishing the net value of S.[8–12] The effectiveness of various approaches to this problem may be measured by the values of S in the electronic ground state.[4,13–19]

† University of Nebraska.

‡ National Center for Neutron Research. Present address: Neutron Scattering Section, ORNL, Bldg 7962, 1 Bethel Valley Rd., P.O. Box 2008, Oak Ridge, TN 37831-6393.

§ National Center for Neutron Research. Present address: Department of Nuclear and Quantum Engineering, Korea Advanced Institute of Science and Technology, 373-1 Gusong-dong, Yusong-gu, Daejon 305−701, Republic of Korea.

(1) Rajca, A.; Wongsriratanakul, J.; Rajca, S. *Science* **2001**, *294*, 1503−1505.
(2) Rajca, A.; Rajca, S.; Wongsriratanakul, J. *J. Am. Chem. Soc.* **1999**, *121*, 6308−6309.
(3) Rajca, A. *Encyclopedia of Polymer Science and Technology*, 3rd ed.; Kroschwitz, J. I., Ed.; Wiley: New York, 2002.
(4) Rajca, A. *Chem.−Eur. J.* **2002**, *8*, 4834−4841.
(5) Rajca, A.; Utamapanya, S. *J. Am. Chem. Soc.* **1993**, *115*, 10688−10694.
(6) Rajca, A.; Rajca, A.; Padmakumar, R. *Angew. Chem., Int. Ed. Engl.* **1994**, *33*, 2091−2093.
(7) Rajca, A.; Rajca, S.; Desai, S. R. *J. Am. Chem. Soc.* **1995**, *117*, 806−816.
(8) Dvolaitzky, M.; Chiarelli, R.; Rassat, A. *Angew. Chem., Int. Ed. Engl.* **1992**, *31*, 180−181.
(9) Fang, S.; Lee, M.-S.; Hrovat, D. A.; Borden, W. A. *J. Am. Chem. Soc.* **1995**, *117*, 6727−6731.
(10) Silverman, S. K.; Dougherty, D. A. *J. Phys. Chem.* **1993**, *97*, 13273−13283.
(11) Kanno, F.; Inoue, K.; Koga, N.; Iwamura, H. *J. Am. Chem. Soc.* **1993**, *115*, 847−850.
(12) Rajca, A.; Rajca, S. *J. Chem. Soc., Perkin Trans. 2* **1998**, 1077−1082.
(13) Nakamura, N.; Inoue, K.; Iwamura, H. *Angew. Chem., Int. Ed. Engl.* **1993**, *32*, 872.
(14) Iwamura, H.; Koga, N. *Acc. Chem. Res.* **1993**, *26*, 346−351.
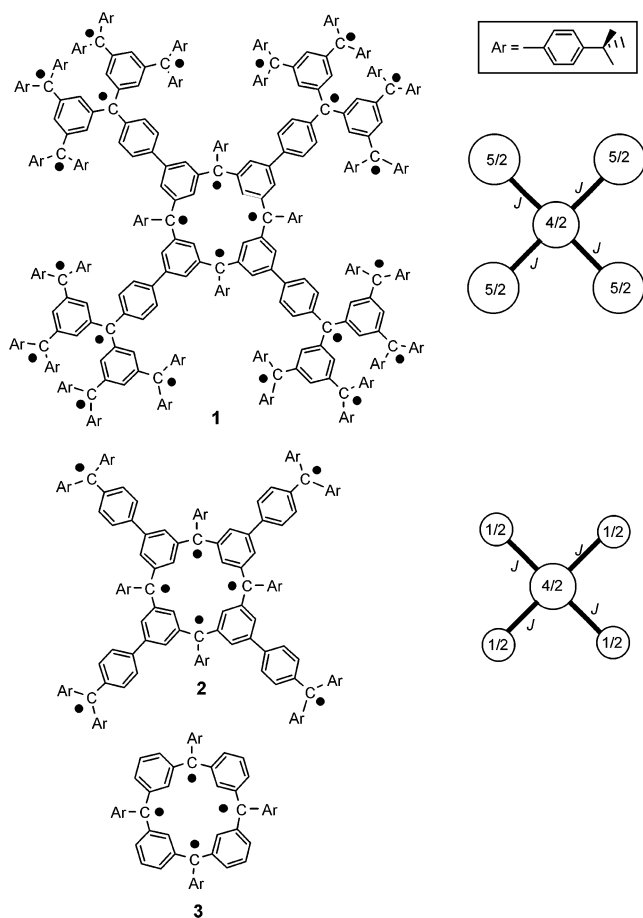(15) Matsuda, K.; Nakamura, N.; Inoue, K.; Koga, N.; Iwamura, H. *Bull. Chem. Soc. Jpn.* **1996**, *69*, 1483−1494.

Figure 1. Target polyradicals **1** and **2** as spin pentamers and tetraradical **3**.

Tetracosaradical (24-radical) **1** and octaradical **2** are designed as "organic spin clusters".[20–22] One of the key elements of this design is the $S = 2$ macrocyclic core, as illustrated by tetraradical **3**.[7] Because ferromagnetic coupling through the 1,3-phenylene moiety is significantly stronger than that through the 3,4′-biphenylene, "unpaired" electrons in the four branches and the macrocyclic core can effectively be lumped into component spins (S').[21,22] Such ferromagnetically coupled $S' = 5/2, 5/2, 5/2, 5/2, 4/2$ spin pentamer should have $S = 12$ ground state; similarly, the $S' = 1/2, 1/2, 1/2, 1/2, 4/2$ spin pentamer should have $S = 4$ ground state (Figure 1).[22]

Another aspect of molecules with large values of S is the magnitude of their magnetic anisotropy barrier. Numerous transition metal ion based molecules (clusters) show substantial barriers for inversion of magnetization, thus acting effectively as "single-molecule-magnets" (SMM) at cryogenic temperatures.[23,24] The magnetic anisotropy of SMM's is primarily based on the single-ion anisotropies, especially of the Jahn–Teller
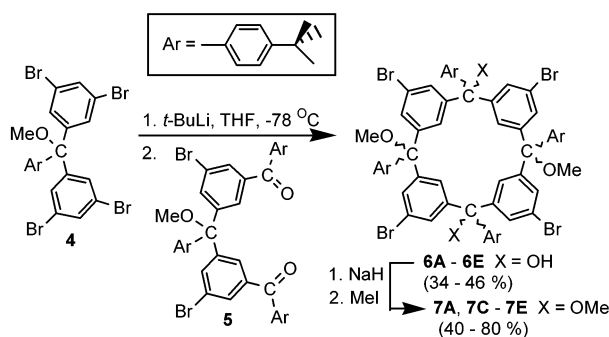
distorted ions.[25] For organic polyradicals, in particular hydrocarbons, the contribution to magnetic anisotropy from the classical magnetic dipole–dipole interactions is expected to be relatively important.[26] Therefore, it might be expected that the barriers for coherent rotation of magnetization in organic polyradicals may be related to the molecular shape of polyradical and its spin density.[4,26,27] Such magnetic shape anisotropies may be significant in polyradicals with elongated shapes.[26,27]

The title 24-radical **1** with $S = 10$, which is the highest spin organic molecule to date,[4,22] provides an excellent model for study of both exchange coupling and the possibility of magnetic shape anisotropy in organic macromolecules. This article describes details of synthesis and characterization of 24-radical **1** and its homologue octaradical **2** (Figure 1), including quantitative magnetic studies. For **1**, shape determinations with small-angle neutron scattering (SANS) are reported. These studies should provide an insight into the magnetic behavior (e.g., related to the magnetic shape anisotropy) in the first conjugated polymer with magnetic ordering.[1,28]

Results and Discussion

1. Synthesis of Polyethers. Modular and convergent synthesis is employed to prepare tetracosaether (24-ether) **1-(OMe)$_{24}$** and octaether **2-(OMe)$_8$**, precursors to 24-radical **1** and octaradical **2**. The synthesis is carried out in two stages: (1) preparation of the tetrafunctionalized macrocyclic module **7E** with an effective C_{4v} point group of symmetry (Scheme 1 and Figure 2); (2) attachment of four monofunctionalized dendritic **8**[21] or monoether **9**[20] modules to the macrocyclic module **7E**, using Negishi coupling (Scheme 2).[29]

Compound **4** and diketone **5** are prepared according to the published procedure.[30] Bis(aryllithium), which is obtained via Li/Br exchange on **4**, is condensed with the diketone **5** to give

Scheme 1. Synthesis of Diols **6** and Tetraethers **7**

(16) Nishide, H.; Ozawa, T.; Miyasaka, M.; Tsuchida, E. *J. Am. Chem. Soc.* **2001**, *123*, 5942−5946.
(17) Michinobu, T.; Inui, J.; Nishide, H. *Org. Lett.* **2003**, *5*, 2165−2168.
(18) Bushby, R. J.; McGill, D. R.; Ng, K. M.; Taylor, N. *J. Chem. Soc., Perkin Trans. 2* **1997**, *7*, 1405−1414.
(19) Anderson, K. K.; Dougherty, D. A. *Adv. Mater.* **1998**, *10*, 688−692.
(20) Rajca, A.; Rajca, S. *J. Am. Chem. Soc.* **1996**, *118*, 8121−8126.
(21) Rajca, A.; Wongsriratanakul, J.; Rajca, S. *J. Am. Chem. Soc.* **1997**, *119*, 11674−11686.
(22) Rajca, A.; Wongsriratanakul, J.; Rajca, S.; Cerny, R. *Angew. Chem., Int. Ed.* **1998**, *37*, 1229−1232.
(23) Lis, T. *Acta Crystallogr., Sect. B* **1980**, *36*, 2042−2046.
(24) Sessoli, R.; Gatteschi, D.; Caneschi, A.; Novak, M. A. *Nature* **1993**, *365*, 141−143.

(25) Boskovic, C.; Pink, M.; Huffman, J. C.; Hendrickson, D. N.; Christou, G. *J. Am. Chem. Soc.* **2001**, *123*, 9914−9915.
(26) Rajca, A. *Chem. Rev.* **1994**, *94*, 871−893.
(27) Aharoni, A. *Introduction to the Theory of Ferromagnetism*, 2nd ed.; Oxford: Oxford, U.K., 2000.
(28) (a) The alternative design of organic spin clusters, addressing the development of net ferri- or ferromagnetic correlations in the conjugated polymer with magnetic ordering, is described in the following: Rajca, A.; Wongsriratanakul, J.; Rajca, S. Organic Spin Clusters: Macrocyclic-Macrocyclic Poly(arylmethyl) Polyradicals with Very High Spin $S = 5−13$. *J. Am. Chem. Soc.* **2004**, *126*, in press. (b) The design annelated macrocyclic organic spin clusters, addressing the dimensionality of the conjugated polymer with magnetic ordering, is described in the following: Rajca, A.; Wongsriratanakul, J.; Rajca, S.; Cerny, R. L. Organic Spin Clusters: Annelated Macrocyclic Polyarylmethyl Polyradicals and Polymer with Very High Spin $S = 6−18$. *Chem.−Eur. J.* **2004**, *10*, in press.
(29) (a) Negishi, E.; King, A. O.; Okukado, N. *J. Org. Chem.* **1977**, *42*, 1821−1823. (b) Negishi, E.; Takahashi, T.; King, A. O. *Org. Synth.* **1987**, *66*, 67−74.
(30) Rajca, A.; Lu, K.; Rajca, S. *J. Am. Chem. Soc.* **1997**, *119*, 10335−10345.
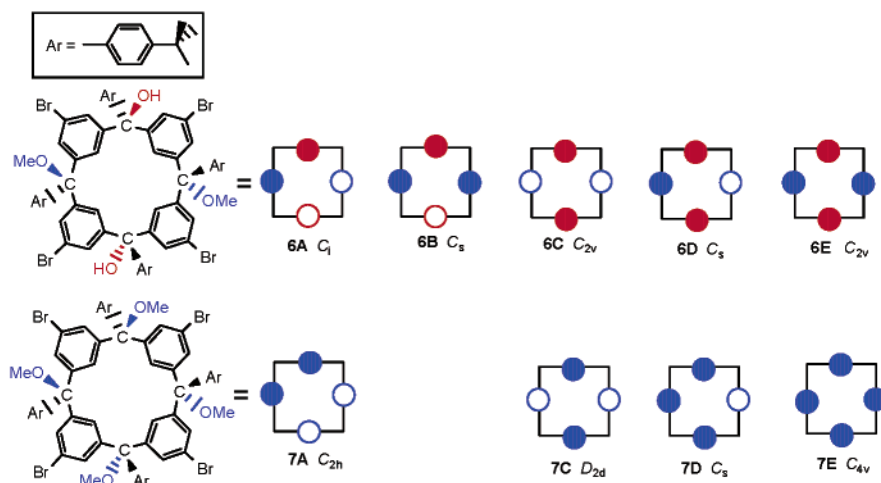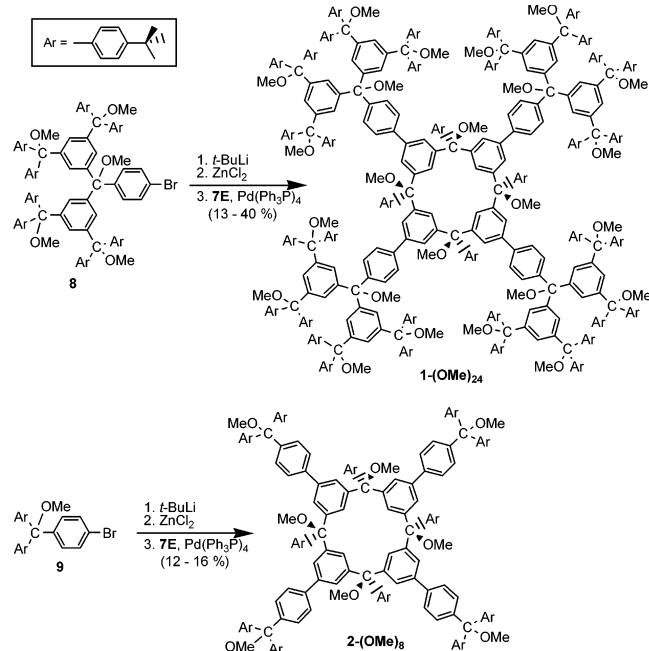
Figure 2. Cis/trans isomers of calix[4]arene diols **6** and tetraethers **7**. Open and closed circles correspond to the relative orientation of the OMe (blue) and OH (red) groups.

Scheme 2. Synthesis of Polyethers **1-(OMe)₂₄** and **2-(OMe)₈**

macrocyclic diols as five cis/trans isomers **6A–E** in overall yield of 34–46% (Scheme 1).

(**6A–E** are labeled alphabetically in the order of increasing polarity on silica.) Although all five possible isomers are isolated, only **6A** (14–17%), **6D** (5–10%), and **6E** (4%) are readily separable on silica; the remaining two isomers are isolated as a mixture of **6B** and **6C** (8–14%, 3.5:1–2.5:1), though small amounts of both isomers are obtained for spectroscopic characterization. Etherification of diols **6A,D,E** with MeI yields the corresponding ethers **7A** (62%), **7D** (63–84%), and **7E** (38–61%); analogously, a mixture of diols **6B,C** (3.5:1) provides a mixture of ethers **7D,C** (88%, 3.6:1), i.e., diols **6B,D** are related to an identical ether **7D**.

All five possible cis/trans isomers of diols **6** and all four possible cis/trans isomers of tetraethers **7** are shown in Figure 2. Their point groups of symmetry, as expected under conditions of fast exchange between different calix[4]arene conformations, are also indicated. For each isomer, FAB MS gives the expected $(M - OCH_3)^+$ cluster ions; the diols **6** show additional, intense

$(M - OH)^+$ cluster ions. Measured and calculated isotopic distributions for both cluster ions show satisfactory agreement. IR spectra show the presence of the OH groups in diols, as two broad peaks (**6A–D**) or one broad peak (**6E**) in the 3400–3600 cm⁻¹ range. The ¹H and ¹³C NMR spectra allow for unambiguous assignment of diols **6A,B,D**, and the corresponding tetraethers **7A,D** (Tables 1s–3s, Supporting Information). However, the most symmetric diols **6C,E** (and the corresponding tetraethers **7C,E**) have similar NMR spectral patterns, precluding their assignment by NMR spectroscopy (Tables 1s–3s, Supporting Information). These two isomer sets are assigned with the help of X-ray crystallography.

The molecular structure from X-ray crystallography of **7E** shows the all-cis isomer; i.e., all four methoxy groups are located on the same face of the macrocycle (Figure 3). This implies that isomer **7C** must have all-trans methoxy groups. Interestingly, the calix[4]arene macrocycle **7E** adopts the 1,3-alternate conformation.[31,32] One of the *tert*-butyl groups is disordered over two positions. The carbon atoms of the *tert*-butyl groups show large displacement parameters, especially C16A–C18A, which are in the vicinity of the solvent void. This suggests the flexibility of the calix[4]arene macrocycle. The inefficient packing of the calix[4]arene results in large voids that contain an unknown amount of solvent (Experimental Section).

The C_{4v}-symmetric isomer **7E**, which shows 4-fold symmetry on the NMR scale at ambient temperature and is readily separable, is selected as the macrocyclic module. Conditions for the Li/Br exchange for the branch module **8** are optimized by isolation of monodeuterated module **8-D** after the MeOD quench of the corresponding aryllithium (Scheme 2). Negishi couplings between the branch modules (**8** and **9**, 6 equiv as organozinc derivatives) and the macrocyclic module (**7E**, 1 equiv) give 24- and 8-ethers **1-(OMe)₂₄** and **2-(OMe)₈** in 13–40 and 12–16% isolated yields, respectively (Scheme 2).

The following side products are isolated: homocoupling products of the branch modules (**10** and **11**, ~10%); debrominated branch module (module **8-H**, 23%); tricoupling product (**12-(OMe)₁₉**, 1%) (Chart 1).

(31) Gutsche, C. D. *Calixarenes Revisited*; RSC, Cambridge, U.K., 1998; Chapter 4.
(32) Rajca, A.; Padmakumar, R.; Smithhisler, D. J.; Desai, S. R.; Ross, C. R.; Stezowski, J. J. *J. Org. Chem.* **1994**, *59*, 7701–7703.
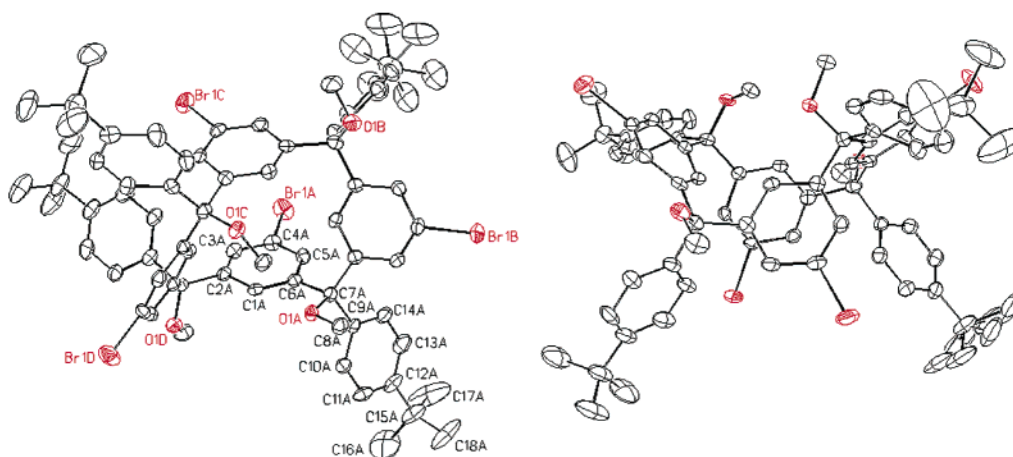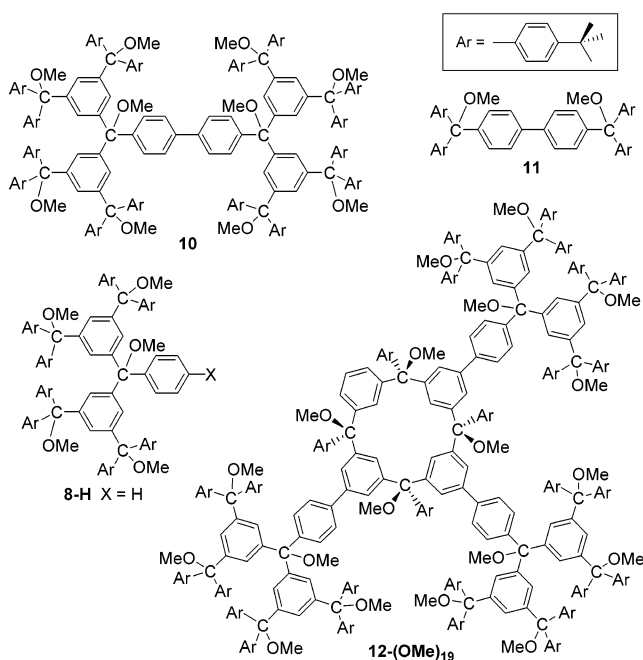
Figure 3. Molecular conformation (two views) for macrocyclic tetraether **7E** as determined by a single-crystal X-ray crystallography. The hydrogen atoms and molecules of solvent of crystallization (benzene) are not shown. Carbon, bromine, and oxygen atoms are depicted with ellipsoids representing the 50% probability level.

Chart 1. Structures of Side Products in Synthesis of **1-(OMe)₂₄** and **2-(OMe)₈**
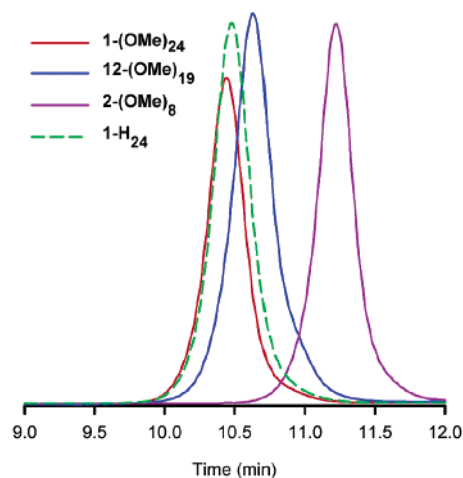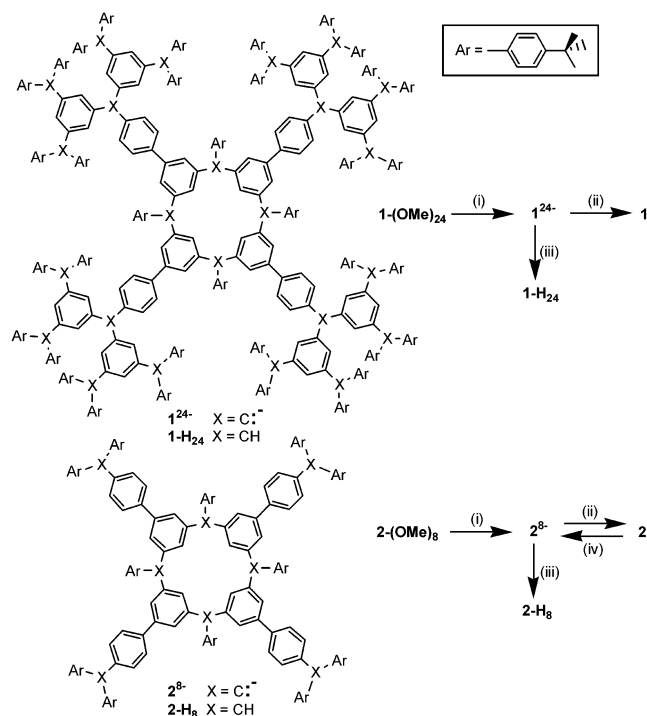

Figure 4. Gel permeation chromatography of **1-(OMe)₂₄**, **1-H₂₄**, **12-(OMe)₁₉**, and **2-(OMe)₈**. Only plots from the refractive index detector are shown.

The target polyethers (and the isolated side products) show expected monocharged $(M - OCH_3)^+$ cluster ions as the most intense signals in the high-mass range of FAB MS (Figure 1s, Supporting Information).[22] The FAB MS for 24-ether **1-(OMe)₂₄**, including the doubly charged $(M - (OCH_3)_2)^{2+}$ cluster ion, was discussed previously.[22]

Gel permeation chromatography (GPC) with multiangle light scattering (MALS) provides another absolute measure of molecular mass and column-dependent measure of monodispersity (or polydispersity). The elution time is decreasing in the order **1-(OMe)₂₄**, **1-H₂₄**, **12-(OMe)₁₉**, and **2-(OMe)₈**, reflecting decreasing hydrodynamic radii for the decreasing molar masses (Figure 4). (The structure of **1-H₂₄** is shown in Scheme 3.) All four compounds are monodisperse, giving PD = 1.00 for the first-order polynomial fit (Table 4s, Figure 2s, Supporting Information). The measured M_w for hydrocarbon **1-H₂₄** is 6.3−6.4 kDa, which is in an excellent agreement with

the formula mass of 6314 g mol⁻¹. For all three polyethers M_w's are overestimated by about 10% (Table 4s, Supporting Information); assuming that only about 90% of the injected mass of polyether is eluted into detectors, good agreement with the formula masses is obtained. Such partial retention on the tetrahydrofuran-eluted GPC column is reasonable in view of the relatively high reactivity of triarylmethyl ethers.

¹H and ¹³C NMR spectra corroborate the expected 4-fold symmetry for 24-ether **1-(OMe)₂₄** and 8-ether **2-(OMe)₈**.[33] The NMR spectra for dendritic fragments of polyethers **1-(OMe)₂₄**, **8-H**, and **10** are best interpreted in terms of two nonequivalent sets of 4-*tert*-butylphenyl groups, analogously to the previously discussed NMR spectra of branch module **8**.[21,33a] In the aromatic region of the ¹H NMR spectra for 24-ether **1-(OMe)₂₄** at 348 K, the expected COSY off-diagonal peaks are observed, except for the two most downfield, broadened resonances at 7.97 (4H) and 7.90 (8H).[22] In the aromatic region the of ¹H−¹³C HMQC spectrum at 348 K, 9 out of 10 expected (assuming insufficient

---

(33) (a) In the *t*-Bu region of **1-(OMe)₂₄**, the ¹H NMR spectrum at 293 K shows three singlets in the expected ratio (16:16:4); at 348 K, the ¹H and ¹³C resonances for the diastereotopic *t*-Bu groups are not resolved. (b) In the MeO-group region of **1-(OMe)₂₄**, three (1:1:4) ¹H resonances are resolved at 293 K.

Scheme 3.[a] Generation of Polyradicals **1** and **2**

$$Ar = \text{[4-tert-butylphenyl structure]}$$

1-(OMe)₂₄ → (i) → **1²⁴⁻** → (ii) → **1**

1²⁴⁻ → (iii) → **1-H₂₄**

1²⁴⁻ X = C:⁻
1-H₂₄ X = CH

2-(OMe)₈ → (i) → **2⁸⁻** → (ii)/(iv) → **2**

2⁸⁻ → (iii) → **2-H₈**

2⁸⁻ X = C:⁻
2-H₈ X = CH

[a] Conditions: (i) Na/K, 283 K for ∼5 d; (ii) I₂, 167–170 K; (iii) MeOH; (iv) Na/K, 178–195 K for several hours.
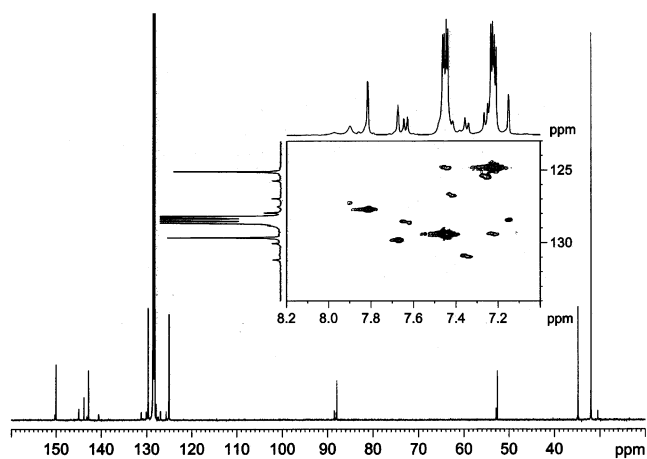

Figure 5. ¹³C NMR (125 MHz, benzene-d_6) spectrum for 24-ether **1-(OMe)₂₄** at 348 K. Main plot: full spectrum. Inset plot: ¹H–¹³C HMQC correlation in the aromatic region.

resolution for diastereotopic 4-*tert*-butylphenyls) cross-peaks are observed; in particular, the ¹H resonance at 7.90 ppm correlates to a broad ¹³C resonance at 127.0 ppm (Figure 5). The absence of the cross-peak to the ¹H resonance at 7.97 ppm corresponds to the missing nonquaternary ¹³C resonance in the aromatic region, which is perhaps too broad to be detected under the present experimental conditions.

In the less sterically congested octaether **2-(OMe)₈**, the most downfield ¹H resonances appear at similar chemical shifts, 8.06 (4H) and 7.95 (8H), and do show off-diagonal peaks in the COSY correlation at ambient temperature (Figure 3s, Supporting Information). Similarly, both downfield ¹H resonances show cross-peaks in the ¹H–¹³C HSQC correlation at ambient temperature, i.e., (8.06, 130.4) and (7.95, 127.5) (Figure 4s, Supporting Information). Therefore, the two most downfield ¹H

resonances in **1-(OMe)₂₄** are assigned to the four 1,3,5-trisubstituted benzene rings of the calix[4]arene core.

2. Generation of Carbopolyanions and Polyradicals. The generation of carbopolyanions and polyradicals is shown in Scheme 3. When polyethers **1-(OMe)₂₄** and **2-(OMe)₈** (0.5–30 mg) are treated with Na/K alloy in THF-d_8 (0.06–0.12 mL), the reaction mixture briefly turns blue and, subsequently, deep purple red or purple blue. After about 5 days at 283 K, the solutions of deep purple red carbopolyanion **1²⁴⁻** and purple blue carbooctaanion **2⁸⁻** are filtered into a SQUID, NMR, ESR, or SANS sample container (Figure 13). Addition of iodine in small portions at 170–167 K leads to a blue, green (or blue gray), and, finally, yellow-brown to red-brown reaction mixture to give polyradicals **1** and **2** (Scheme 3).[34]

Unlike previously studied low molecular weight carbopolyanions, which typically possessed well-resolved NMR spectra,[7,34a,35] **1²⁴⁻** has broadened ¹H NMR spectra in the 293–193 K range, preventing peak assignment. The broadening of the resonances is reversible and increases significantly at low temperatures. (The solutions of **1²⁴⁻** appear as more viscous compared to the solutions of the corresponding 24-ether **1-(OMe)₂₄** and 24-radical **1**.) The ¹³C NMR spectrum at 293 K shows fewer than expected, relatively broad resonances (Figure 6).

The ¹³C resonance at 85.8 ppm is in the chemical shift range of the triarylmethyl carbons in analogous carbopolyanions.[34a,35] Moreover, no resonances corresponding to methoxy carbons are detected. Addition of MeOH to carbopolyanion **1²⁴⁻** gives the isomeric mixture of the corresponding hydrocarbon **1-H₂₄**. Similarly, hydrocarbon **2-H₈** is obtained, when octaradical **2** is treated with Na/K alloy at 178–195 K, and then the resultant carbopolyanion is quenched with MeOH.

FAB MS for poly(arylmethyl) hydrocarbons are relatively difficult to obtain, compared to the corresponding polyethers.[21] The expected molecular ion for **2-H₈** is detected with the signal-to-noise of only 2–3, and for much larger **1-H₂₄**, no molecular ion is found in FAB MS. However, GPC MALS of **1-H₂₄** in THF gives values of M_w that are in excellent agreement with the formula molecular mass. Furthermore, molecular size as measured by radius of gyration (see section on SANS studies) for **1-H₂₄** is similar to that for 24-ether **1-(OMe)₂₄**. The ¹H NMR integrations of the aromatic, Ar₃CH, and *tert*-butyl regions are in good agreement with the expected ratio of 196:24:324 for hydrocarbon **1-H₂₄**; the ¹³C NMR spectrum shows the expected resonances for Ar₃CH in the 56–57 ppm region. Both NMR and IR spectra indicate the absence of the arylmethyl ether linkages.

3. Magnetic Studies of Polyradicals. 3.1. ESR Spectroscopy. The CW X-band ESR spectrum of octaradical **2** in THF-d_8/2-methyltetrahydrofuran at 77 K shows only one unresolved resonance in both $\Delta m_s = 1$ and $\Delta m_s = 2$ regions. It is expected that the spectrum possesses too many closely spaced lines to be resolved. The $\Delta m_s = 1$ region for the previously studied 1,3-phenylene-based octaradical also showed a broad resonance, and only 12 (out of expected 16) barely resolved shoulders have been tentatively assigned to the $S = 4$ ground state with axial zero field splitting parameter $|D/hc| \approx 0.001\,27$ cm⁻¹.[7] The

(34) (a) Rajca, A. *J. Am. Chem. Soc.* **1990**, *112*, 5889–5890. (b) Rajca, A. *J. Am. Chem. Soc.* **1990**, *112*, 5890–5892.
(35) NMR spectroscopy of triarylmethyl-based carbopolyanions: (a) Utamapanya, S.; Rajca, A. *J. Am. Chem. Soc.* **1991**, *113*, 9242–9251. (b) Rajca, A.; Utamapanya, S. *J. Org. Chem.* **1992**, *57*, 1760–1767.
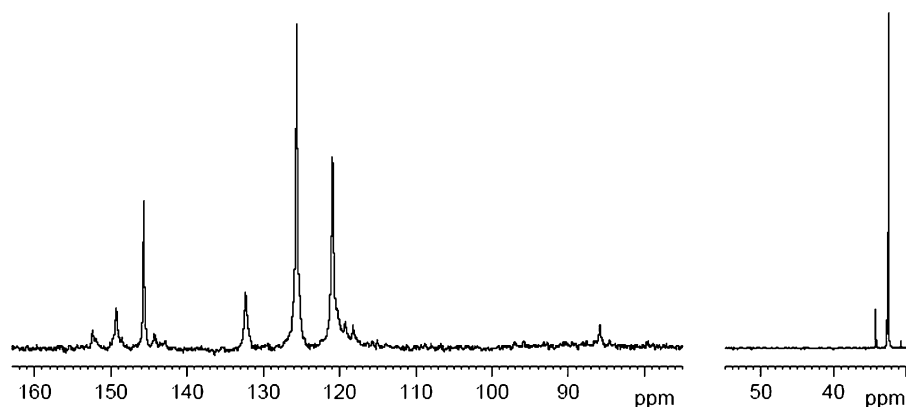
Figure 6. ^{13}C NMR (125 MHz, THF-d_8) spectrum for carbopolyanion **1^{24-}**. Exponential line broadenings of 10 and 1 Hz are applied to the downfield (relative scale of 12) and upfield (relative scale of 1) parts of the spectrum, respectively.

presence of the biphenylene moieties in **2** is expected to increased delocalization of spin density in **2** compared to the 1,3-phenylene-based octaradical.[6] This suggests relatively small values of the predominant magnetic dipole-based contribution to $|D/hc|$.[20,21,36−38] Consequently, the ESR resonances in the $S = 4$ state of **2** may be about 2−3 times more densely spaced within the spectral width of $14|D/hc|$, leading to an unresolved spectrum. In addition, the thermal population of the low-spin excited states (see bulk magnetization and magnetic susceptibility studies) may further complicate the ESR spectrum at 77 K. Because the spectral width is approximately constant within the homologous series of poly(arylmethyls), resonances in the CW ESR spectra become rapidly more congested with increasing values of S (number of resonances increases as $4S$ or $6S$ depending on symmetry). Therefore, bulk magnetic susceptibility and magnetization studies are techniques of choice for determination of large values of S.[39,40]

3.2. Bulk Magnetic Susceptibility and Magnetization Studies. For magnetic studies, samples of polyradicals **1** and **2** are typically prepared from 0.5 to 1.8 mg of polyethers **1-(OMe)$_{24}$** and **2-(OMe)$_8$** in THF-d_8 (0.06−0.08 mL). Special care is taken to ensure accurate weight for the polyethers.[41] Magnetization (M) is measured as a function of magnetic field ($H = 0−50$ kOe) and temperature ($T = 1.8−150$ K) for **1** and **2** in THF-d_8. For selected samples, the following sequences of measurements is carried out: first, without annealing (with sample chamber degassed at 90 K); second, with prior annealing at 170 K (slightly above the melting point of the matrix); third, after exposure of the sample to room temperature for about 0.5 h.

For the most dilute samples of **1** (∼0.002 M) and **2** (<0.005 M), the M vs H data at 1.8, 3, 5, and 10 K are numerically fit to one Brillouin function ($B(S)$),[42] with spin (S) and magnetization at saturation (M_{sat}) as variable parameters (Tables 1 and 2). The values of $S = 9.8$ and $S = 3.8$ are obtained for **1** and

Table 1. Summary of Magnetic Data for 24-Radical **1**

| sample label | mass (mg) | anneal (K) | One-Brillouin | | Two-Brillouin | | M_{sat}^{a} (μ_B) | χT_{max}^{b} | J/k (K) |
			S	−Θ (K)	S_s	−Θ (K)			
1087^c	1.50	90	10.0	0.03			0.70	46.6	6.6^d
		170	10.5	0.3			0.71		6.5^d
		293	2.8	0.25			0.18	3.8	
1109	1.26	90	9.8	0	9.9	0	0.54	35.8	6.9^d
		170	9.8	0			0.53	35.4	7.1^d
1756	1.54	90	10.0	0.05	10.0	0.05	0.63	43.0	7.3^e
		170	10.0	0.05	10.1	0.05	0.63	44.6	7.7^e
		293	3.3	0.1	3.3	0.1	0.24	6.2	
1911^f	0.50	90			8.2	0	0.46	26.6	7.5^e
1923	1.13	170	9.6	0.1	9.7	0.1	0.60	38.3	7.2^e

^{a} M_{sat}/mol of triarylmethyl ether. ^{b} χT_{max}/mol of 24-ether **1-(OMe)$_{24}$**. ^{c} Point-by-point correction for diamagnetism, except for samples 1911 and 1923. ^{d} At 5000 Oe. ^{e} At 500 Oe. ^{f} Polyradical preparation at $T > 170$ K.

2; the M/M_{sat} vs H/T plots are nearly overlapping with the $S = 10$ and $S = 4$ Brillouin functions, respectively (Figure 7). The observed temperature dependence of S is consistent with an ideal paramagnet behavior for dilute samples of **1** and **2** below 5 K. For more concentrated samples of **1** and **2**, the additional mean-field parameters (Θ) are used to correct for small intermolecular antiferromagnetic (Θ < 0) interactions. Numerical fits to modified Brillouin functions, M vs $H/(T − Θ)$, with Θ = −0.03 or −0.05 K, give $S = 10.0$ at 1.8, 3, and 5 K and $S = 9.8$ at 10 K for **1**. For **2**, $S = 3.6$ ($|Θ| = 0.1−0.2$ K) at 1.8, 3, and 5 K are obtained (Tables 1 and 2).[43]

Additional numerical fits of the M vs H data for **1** are carried out with linear combination of two Brillouin functions, $B(S)$ and $B(1/2)$, using three variable parameters: S, M_{sat}, and w (eq 1).

(36) The zero field splitting parameter ($|D|$) vs the interdipole distance in diradicals: Rohde, O.; Van, S. P.; Kester, W. R.; Griffith, O. H. *J. Am. Chem. Soc.* **1974**, *96*, 5311−5318.
(37) The values of $|D/hc|$ (cm^{-1}) for 3,4′-biphenylene-based di-, tri-, and pentaradicals are smaller by a factor of about 2−3, compared to their 1,3-phenylene counterparts, e.g., for 3,4-′biphenylene- vs 1,3-phenylene-based polyradicals:[20,21] 0.0025 vs 0.0066 (diradicals); 0.0016 vs 0.004−0.006 (triradicals); 0.0016 vs 0.0027 (pentaradicals).
(38) Minato, M.; Lahti, P. M.; van Willigen, H. *J. Am. Chem. Soc.* **1993**, *115*, 4532−4539.
(39) Rajca, A.; Utamapanya, S.; Thayumanavan, S. *J. Am. Chem. Soc.* **1992**, *114*, 1884−1885.

(40) In the most favorable case of the $|E/hc|$, polyradical with $S = 12$ would possess 48 resonances in the $\Delta m_s = 1$ region; with the expected spectral width of the order of 0.006 cm^{-1}, only a broad single line would be observed. The spectral width, due to the magnetic dipole−dipole couplings, may be significantly greater (elongated or flat shapes) or smaller (spherical-like shapes) than 0.006 cm^{-1}.
(41) (a) The weighed amount of polyether must be viewed as an upper bound for the actual amount used for generation of polyradical because of the difficulty in quantitative transfer of electrostatic powder in to the reaction vessel. (b) One sample of **2** is prepared on a 9.4-mg scale for SQUID-measurement-followed-by-quenching experiment (Table 2, entry 1).
(42) Carlin, R. L. *Magnetochemistry*; Springer: Berlin, 1986.
(43) The mean-field correction with parameter Θ, as implemented here, provides an approximate description of small exchange couplings, in particular intermolecular antiferromagnetic couplings in more concentrated solutions. Such a description is valid as long as $|Θ|$ is relatively small compared to the studied temperature range. The origin of the large value of $|Θ| = 0.25$ K, shown by one sample of **1** after annealing at 170 K (Table 1, entry 1), is not known. The increased values of $|Θ|$ for the lower molecular weight polyradicals (**2** vs **1**) follow the previously observed trends (e.g., ref 21).

Table 2. Summary of Magnetic Data for Octaradical **2**

| | | | | Numerical Fits | | | | | |
| | | | | Brillouin | | | Heisenberg Hamiltonian | | |
sample label[c]	mass (mg)	concn (M)	anneal (K)	S	$M_{sat}{}^{a}$ (μ_B)	$-\Theta$ (K)	J/k (K)	$-\Theta$ (K)	$\chi T_{max}{}^{b}$ (emu K mol^{-1})
Suk98[d]	na	<0.005	90	3.8	na	0.0	na	na	na
Sul13	1.50	0.008	90	3.6	0.77	0.2	33	0.15	
			170	3.6	0.76	0.2	34	0.16	7.0
1138	1.64	0.011	90	3.5	0.81	0.2	37	0.14	7.3
Sul08[e]	<1.8	<0.01	90	3.6	na	0.1	30	0.06	na

[a] M_{sat}/mol of triarylmethyl ether. [b] χT_{max}/mol of octaether **2-(OMe)$_8$**. [c] Point-by-point correction for diamagnetism, except for sample Sul08. [d] 0.009 M octaradical **2** prepared from 9.4 mg of octaether in the old-style generation vessel and then further diluted. [e] Preparation in glovebox.
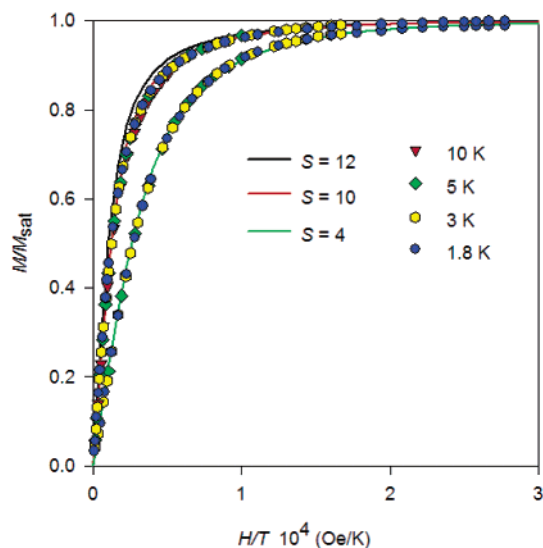

Figure 7. SQUID magnetometry ($H = 0-50$ kOe) for dilute solutions of polyradicals **1** (0.002 M, sample label 1109) and **2** (<0.005 M, sample label Suk98) in THF-d_8. Experimental points at $T = 1.8$, 3, 5, and 10 K and Brillouin functions with $S = 4$, 10, and 12 are shown, as symbols and lines, respectively. Numerical fitting to Brillouin function, using two variable parameters (S and M_{sat}), gives $S = 9.8$ and 3.8 for **1** and **2**, respectively, at 1.8, 3, and 5 K. At 10 K, $S = 9.6$ is obtained for **1**. The parameter dependencies are 0.26–0.72 and 0.32–0.74 for **1** and **2**, respectively. All experimental data here are plotted after point-by-point correction for diamagnetism.

Figure 8. Plots of χT vs T for concentrated solutions of polyradicals **1** (0.003 M, sample label 1756) and **2** (0.008 M, sample label Sul13) in THF-d_8. The symbols and lines are the experimental points and numerical fits to the spin-pentamer models, respectively. For **1** at $H = 500$ Oe, the fitting parameters and their parameter dependencies are $J/k = 7.7$ K (0.46) and $N = 1.16 \times 10^{-7}$ mol (0.46); for **2** at 5000 Oe, $J/k = 33.8$ K (0.59), $N = 4.17 \times 10^{-7}$ mol (0.76), and $\Theta = -0.16$ K (0.62) are obtained. All experimental data here are obtained after annealing at 170 K and point-by-point correction for diamagnetism.

The $S = ^1/_2$ Brillouin function ($B(1/2)$) may account for some of the polydispersity in the value of S. Parameter w is a measure of relative contribution from different Brillouin functions to overall M. Taking into account that contribution to overall M from each Brillouin function has to be effectively multiplied by its value of S,[42] w is dependent on another variable parameter S, as well. Consequently, values of spin-weighed average spin (S_s) are calculated using the following expression: $S_s = (S + 0.5w)/(1 + w)$. Addition of the third variable parameter somewhat improves the numerical fits, though the values of S_s are very similar to the values of S obtained from one-Brillouin fits (Table 1). This may suggest that the amount of the impurities, with very low values of S, is relatively insignificant.[44]

$$M = M_{sat}[(B(S) + wB(1/2))]/(1 + w) \qquad (1)$$

The M vs T data at $H = 5000$, 500, and 50 Oe are plotted as the product of magnetic susceptibility per mol of starting polyether ($\chi = M/H$) and temperature vs temperature, i.e., χT vs T (Figure 8). For both **1** and **2**, the values of χT are increasing with decreasing temperature, indicating the thermal depopulation of the low spin excited states, i.e., suggesting the presence of a
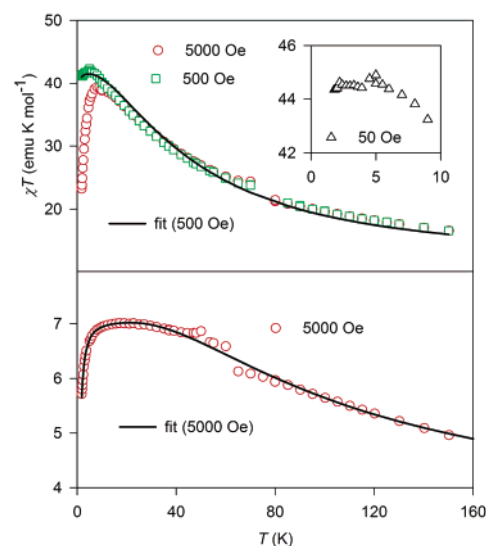
weak ferromagnetic coupling. At low temperatures and modest magnetic fields ($H = 5000$ Oe), the downward turn in χT is predominantly, if not exclusively, associated with the paramagnetic saturation. Ideal paramagnetic behavior (flat χT vs T plot) is established for **1** at $T \leq 5$ K, using low magnetic fields ($H = 50$ Oe) (Figure 8, inset).

The χT vs T dependence is fit to a model on the basis of a pentamer of four spin carriers with $S = 5/2$ (for **1**) or $S = 1/2$ (for **2**) ferromagnetically coupled to one with a spin of $S = 4/2$.[22] Energy eigenvalues for Heisenberg Hamiltonian are obtained by vector decoupling technique.[45–48] For **2**, only relatively concentrated solutions are used for the χT vs T fits; this provides adequate signal-to-noise, especially in the higher temperature range, where the overall magnetic moment of the sample is diamagnetic. Equations for magnetization, including saturation effects, are derived using standard formulas.[47,48]

(44) For **1** at 1.8 and 2.5 K, the maximum value of the parameter dependence in the numerical fits to eq 1 does not exceed 0.91 (Table 1).
(45) Heisenberg, W. *Z. Phys.* **1928**, *49*, 619−636.
(46) Beloritzky, E.; Fries, P. H. *J. Chim. Phys. (Paris)* **1993**, *90*, 1077−1100.
(47) Rajca, A. In *Hyper-structured Molecules III*; Sasabe, H., Ed.; Gordon and Breach: Reading. U.K., 2001; Chapter 3, pp 46−60.
(48) Rajca, A. *Mol. Cryst. Liq. Cryst.* **1997**, *305*, 567−577.

Numerical fits use J/k (spin coupling constant in Kelvin) and N (number of moles of polyradical), as variable parameters. $J/k = 7 \pm 1$ K and $J/k = 34 \pm 4$ K, corresponding to a pairwise ferromagnetic couplings of spins 5/2 to 4/2 and 1/2 to 4/2, respectively, through 3,4′-biphenylene moiety, are obtained (Figure 8, Tables 1 and 2). For such values of J/k, it is calculated that both **1** and **2** should behave as ideal paramagnets at $T \leq 5$ K; i.e., their $S = 12$ and $S = 4$ ground states are nearly completely populated.[49] This is consistent with a flat χT vs T plot at low magnetic fields, such as 50 Oe for **1** in the inset of Figure 8.[50]

Although χT vs T plots fit reasonably well to the pentamer models for both **1** and **2**, the values of S from the curvatures of Brillouin functions (M vs H/T plots) are somewhat below the theoretical values of $S = 12$ for ferromagnetically coupled 24 unpaired electrons in **1** and $S = 4$ for ferromagnetically coupled 8 unpaired electrons in **2**, respectively. For the quantitative values of M_{sat} and χT, based upon the amount of polyethers weighed for polyradical generation, the discrepancy between the experiment and the theory is even greater. This may in part arise from incomplete transfer of samples of polyethers, which are highly electrostatic powders, to the reaction vessel, mass losses at the stage of filtration of carbopolyanion, or chemical defects in generation of polyradicals.

For quantitative conversion of polyethers to ferromagnetically coupled polyradicals **1** and **2**, χT_{max} should reach 78 and 10 emu K mol^{-1}, respectively. However, the maximum values of χT are only about 45 and 7 emu K mol^{-1} for **1** and **2**, respectively.

M_{sat} measures the number of unpaired electron spins (or spin concentration) in the limit of low temperature and high magnetic field. For the best samples of **1**, M_{sat} is about $0.6-0.7$ μ_B/arylmethyl; i.e., $60-70\%$ of the expected value for quantitative conversion of **1-(OMe)$_{24}$** to **1** with 24 unpaired electrons. Analogous percentages for **2** are somewhat higher at about 80%. The values of M_{sat} for **1** imply that only $14-17$ electron spins are effectively present in an average molecule of **1** within the limit of low T and high H. How could this relatively small number of radicals ($S = {}^1\!/_2$) lead to relatively high value of $S = 10$ for **1**? Analogous question arises for **2**. Such discrepancies may in principle be reconciled, considering that both M_{sat} and S are different averages for polydisperse spin systems. M_{sat} corresponds to a number average; S, as fit to the curvature of the Brillouin function, is approximately a weighed average (S_s).[51] For polydisperse systems, weighed average may be significantly greater than the corresponding number average. Furthermore, M_{sat} may be underestimated by incomplete mass balance, as mentioned in the preceding paragraphs.[41a]

In the preliminary report, only qualitative magnetic data for **1** were available.[22] The discrepancy between the theoretical value of $S = 12$ and the experimental value of $S = 10$, obtained from the curvature of the Brillouin plot, was ascribed to the presence of small and randomly distributed density of chemical defects.[22] The corresponding percolation model (Experimental Section) gives density of chemical defects at the level of about 2%.[22,51] Such defects may result from less than 100% yield for generation of "unpaired" electrons or synthetic impurities in polyether precursors. However, $M_{sat} = 0.6-0.7$ μ_B would correspond to the density of chemical defects in the $30-40\%$ range; this would imply highly nonstatistical (rather than random) distribution of chemical defects, with the predominant density of defects at the 16 terminal triarylmethyl sites. Because of low temperatures employed for measurement of M_{sat}, antiferromagnetic interactions may contribute to the low values of M_{sat}. For example, antiferromagnetic exchange coupling arising from a near 90° twisting of one of the biphenyls (at the phenyl−phenyl CC bond) would lead to cancellation of 10 electron spins; i.e., $M_{sat} = 14$ μ_B/24 ≈ 0.58 μ_B and $S = 7$. Analogously, two such twistings, would give polyradical with $M_{sat} = 4$ μ_B/24 ≈ 0.17 μ_B and $S = 2$. A mixture of conformers with 0, 1, and more twistings could qualitatively account for the experimentally found averages for M_{sat} and S.[52]

Thermal Stability (Persistence) of Polyradical 1. Annealing at 170 K (just above the melting point of the matrix) for a few minutes does not affect the results for two samples of **1**; however, the third sample shows increased values of S and $|\Theta|$ after after annealing (Table 1). For two samples, magnetic moment is continuously measured at 170 K for 12+ h. The sample, which is somewhat overtitrated with iodine, shows a slow decrease of moment over time. However, the other sample possesses unchanged magnetic moment after 12+ h at 170 K, suggesting that polyradical **1** is persistent (stable) at 170 K. Two samples of **1** are annealed at room temperature for 30 min, and subsequently, repeat magnetic studies are carried out (Table 1). For both samples, the values of $S \approx 3$ are obtained, i.e., about 30% of the original value. Similar relative decreases are observed for values of M_{sat} (Table 1).

Conformational Searches. Monte Carlo conformational searches for polyradical **1** provided low-energy conformations with elongated shapes with overall dimensions of $4 \times 3 \times 2$ nm (Figure 9). As shown by the color coding for polyradical **1** in Figure 9, the core calix[4]arene adopts a 1,3-alternate conformation. Consequently, each pair of the diagonally positioned dendritic branches occupies the opposite faces of the core calix[4]arene. The conformation of polyradical **1** has an approximate D_{2d} symmetry; the two pairs diagonally positioned dendritic branches are interchangeable by the S_4 axis, collinear with the C_2 axis of the molecule (Figure 9).

Monte Carlo conformational searches for tetraradical **3** give the analogous 1,3-alternate conformations for the lowest energy structures. In **3**, the eight CCCC torsional angles along the inner macrocyclic carbon backbone of the calix[4]arene core are moderate, at about 47°, consistent with the $S = 2$ ground state found in THF (or 2-MeTHF/THF) matrixes.[7] However, in **1**, the analogous torsional angles are in the 40−70° range, e.g., 63, 47, 72, 42, 55, 49, 67, and 49°. Such conformations should

(49) Equations for $M(T,H)$ derived from Heisenberg Hamiltonians for the spin pentamers are used.

(50) The energy gaps between the ground state and the lowest excited state are identical in units of J/k for both spin pentamers, i.e., $4J/k$. The overall span of energy levels is $20J/k$ (680 K) and $84J/k$ (588 K) for pentamers corresponding to **1** and **2**, respectively. For reliable calculation of thermal behavior, all energy levels, including multiplicities and m_s sublevels, should be taken into account.

(51) Number average S_n in refs 2 and 22 should be replaced with weighed average S_s.

(52) A percolation model for **1**, in which random distribution of chemical defects and random distribution of ferromagnetic vs antiferromagnetic couplings across the four biphenylene moieties are assumed, is developed (eq 5, Experimental Section). Analogous percolation models are described in detail in ref 28a. However, the numerical fits of the M vs H/T data to such models are not satisfactory. Possibly, steric congestion of the dendritic branches in **1**, as found in conformational searches, affects the distribution of conformations, leading to nonrandom distribution of exchange couplings across biphenylene coupling units.
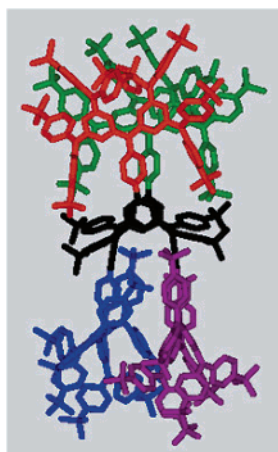
Figure 9. Low-energy conformation for polyradical **1** that is obtained using Monte Carlo conformational searches with the MM2* force field (Macromodel 6.5).

still be compatible with the ferromagnetic coupling for the four unpaired electrons in the macrocyclic core of **1**.[10,53]

The torsional angles, involving 1,3-phenylene moieties within the dendritic branches, are in the 20–57° range; however, the higher angles (e.g., above 47°) are found only at the periphery of the dendritic branch. The torsional angles for the biphenyl moieties in **1** are typically about 48° for the lowest energy conformations. However, conformations, in which one of the biphenyls has a torsional angle approaching 90°, are at ~8 kcal/mol relative to the lowest energy conformations. Severe twisting of the biphenyl moiety does not appear to affect significantly the overall molecular shape of **1**.

Conclusions about the exchange coupling based upon calculated conformations must take into consideration that it is not absolutely certain whether the conformation associated with the global minimum was found and whether the calculated conformations in the gas phase represent adequately those in THF-d_8 frozen solutions.[54] With these precautions in mind, the lowest energy conformations of **1** are probably compatible with ferromagnetic coupling; the somewhat higher in energy conformations may have antiferromagnetic coupling between the dendritic branch and the macrocyclic core.

The calculated, dumbbell-like molecular shapes for **1** have overall sizes exceeding 1 nm making possible their experimental verification using small-angle scattering techniques.[55]

Small-Angle Neutron Scattering. Solutions of polyradical **1**, 24-ether **1-(OMe)₂₄**, hydrocarbon **1-H₂₄**, and carbopolyanion **1²⁴⁻** in THF-d_8 are studied with small-angle neutron scattering (SANS).

Polyradical **1** is handled at temperatures ≤170 K at all times to prevent any substantial decomposition. This poses technical problems for obtaining the SANS data of high quality: (1)

(53) For each 1,3-phenylene moiety of the macrocyclic core of **1**, at most one torsional angle is relatively large near 70°, with the other torsional angle approaching 50°. Severe twisting on one side of 1,3-phenylene moiety does not appear to lead to antiferromagnetic coupling, e.g., ref 10.

(54) There is no detailed quantitative data on the dependence of the exchange coupling vs torsional angles in either 1,3-phenylene or 3,4′-biphenylene moieties. However, a "Karplus–Conroy-type" relationship for exchange coupling in trimethylene-based bis(semiquinone) diradicals was proposed: Shultz, D. A.; Fico, R. M., Jr.; Bodnar, S. H.; Kumar, K.; Vostrikova, K. E.; Kampf, J. W.; Boyle, P. D. *J. Am. Chem. Soc.* **2003**, *125*, 11761–11771.

(55) Roe, R. J. *Methods of X-ray and Neutron Scattering in Polymer Science*; Oxford University: New York, 2000; Chapter 5.
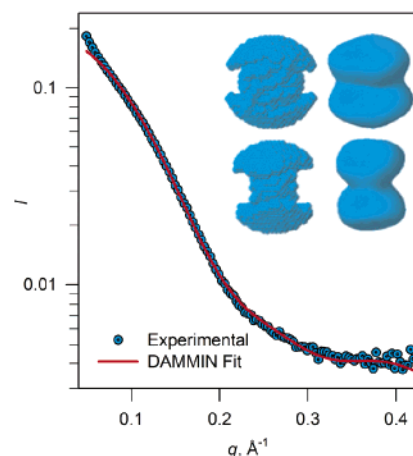
Figure 10. Main plot: SANS intensity (I) vs momentum transfer ($q = 0.049$–0.419 Å^{-1}) for 9×10^{-4} M polyradical **1** (sample label 1907) in THF-d_8 at 170 K. The symbols and solid line correspond to the experimental data points and the numerical fit using GNOM/DAMMIN simulated annealing ($\chi = 4.712$), respectively. Inset: Low-resolution particle shape reconstruction for **1** obtained from the GNOM/DAMMIN fit. Two side views (rotated by 90°), using both the DAMMIN spheres and the spherical harmonics-based envelopes, are shown.
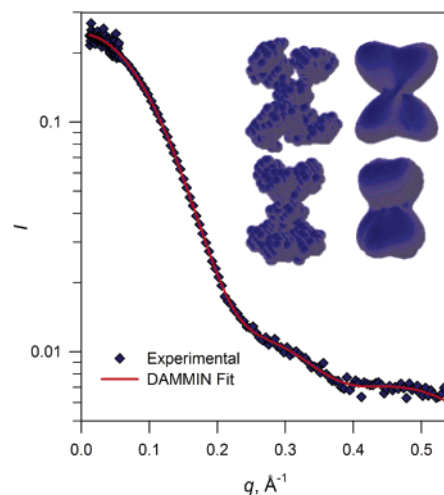
Figure 11. Main plot: SANS intensity (I) vs momentum transfer ($q = 0.012$–0.534 Å^{-1}) for 1.6×10^{-3} M 24-ether **1-(OMe)₂₄** in THF-d_8 at room temperature. The symbols and solid line correspond to the experimental data points and the numerical fit using GNOM/DAMMIN simulated annealing ($\chi = 1.020$), respectively. Inset: Low-resolution particle shape reconstruction for **1-(OMe)₂₄** obtained from the GNOM/DAMMIN fit. Two side views (rotated by 90°), using both the DAMMIN spheres and the spherical harmonics-based envelopes, are shown.

formation of frozen moisture or frozen organic solvent on the outside wall of the sample cell; (2) incomplete melting of the frozen sample solution or inadvertent particles (e.g., precipitate) inside the sample cell. Either of these two problems will lead to an excess of SANS intensity, especially in the low-q range. Elaborate procedures for the sample preparation and handling are developed as described in the Supporting Information.

The logarithmic plots of SANS intensity (I) vs momentum transfer (q) for polyradical **1**, 24-ether **1-(OMe)₂₄**, and hydrocarbon **1-H₂₄** are shown in Figures 10–12. The numerical fits to the SANS data are obtained using the simulated annealing approach of Svergun, as implemented in GNOM/DAMMIN software packages.[56,57] Representative reconstructions of low-resolution particle shapes in the insets of Figures 10–12 are
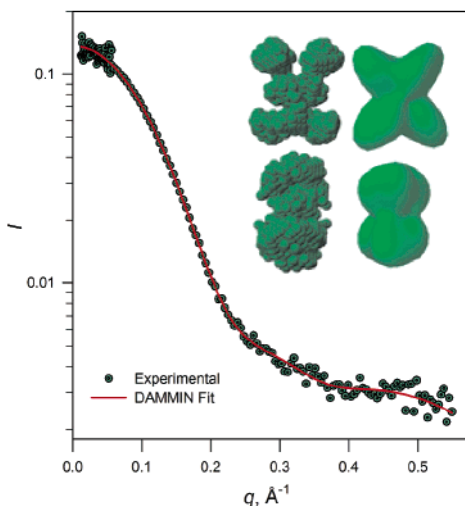
Figure 12. Main plot: SANS intensity (I) vs momentum transfer ($q = 0.012-0.549$ Å^{-1}) for 1.1×10^{-3} M hydrocarbon **1-H$_{24}$** in THF-d_8 at room temperature. The symbols and solid line correspond to the experimental data points and the numerical fit using GNOM/DAMMIN simulated annealing ($\chi = 1.109$), respectively. Inset: Low-resolution particle shape reconstruction for **1-H$_{24}$** obtained from the GNOM/DAMMIN fit. Two side views (rotated by 90°), using both the DAMMIN spheres and the spherical harmonics-based envelopes, are shown.

illustrated using both DAMMIN spheres and spherical harmonics envelopes (up to 6th order); two orientations, related by rotation of about 90° with the respect to the long axis of the molecule, are shown. The spherical harmonics are employed to smooth out the excessive detail of the DAMMIN shapes.[58] The radii of gyration (R_g) for these shapes are 1.5 nm (for **1**) and 1.4 nm (for **1-(OMe)$_{24}$** and **1-H$_{24}$**). Guinier law analysis,[59] which does not consider any particular shape, gives identical values of R_g for **1-(OMe)$_{24}$** and **1-H$_{24}$**. For **1**, Guinier law analysis is not carried because of excess of I, especially in the low-q range. The cause for this excess of I in all samples of **1** is not known. However, this excess of I leads to large values of χ^2 in the DAMMIN fits, though the information concerning molecular shape is contained primarily at the relatively high-q values.[60]

Overall shapes for **1**, **1-(OMe)$_{24}$**, and **1-H$_{24}$** have some similarity to a dumbbell (large on the top and the bottom with the narrow middle part). The experimental resolution of the SANS experiment hardly allows for more detailed description of the reconstructed shape.[60,61] Such a general "dumbbell-like" description also applies to the lowest energy conformations of **1** found by conformational searches (Figure 9).

(56) (a) GNOM: Svergun, D. I. *J. Appl. Crystallogr.* **1992**, *25*, 495−503. (b) DAMMIN: Svergun, D. I. *Biophys. J.* **1999**, *76*, 2879−2886. (c) Svergun, D. I. *J. Appl. Crystallogr.* **2000**, *33*, 530−534. (d) Svergun, D. I.; Stuhrman, H. B. *Acta Crystallogr., Sect. A* **1991**, *47*, 736−744.
(57) Several approaches to reconstruction of three-dimensional solution structures of macromolecules (proteins) from one-dimensional small-angle scattering data are available; however, the ab initio approach, based upon Svergun's simulated annealing GNOM/DAMMIN programs, appears to give the best results, e.g.: Zipper, P.; Durchschlag, H. *J. Appl. Crystallogr.* **2003**, *36*, 509−514.
(58) CRYSOL: Svergun, D. I.; Barberato, C.; Koch, M. H. J. *J. Appl. Crystallogr.* **1995**, *28*, 768−773.
(59) Guinier law: (a) Reference 55, pp 167−174. (b) Guinier, A.; Fournet, G. *Small Angle Scattering of X-rays*; Wiley: New York, 1955.
(60) Resolution of SANS scales with $2\pi/q$.
(61) Because the shapes in this size range close to 1 nm is determined at relatively high q, there is a possibility for the interference from the internal structure and the solvent structure. For **1**, the excess of I, which is found at low q, may tail into the high-q region, leading to further decrease in reliability of the shape reconstruction.

One of the samples of **1** is allowed to attain room temperature for about 4 min. Following cleaning of outside windows of the sample cell at room temperature, the sample is reinserted to the cryostat and the SANS data are collected at 170 K again. The excess of I is still visible at low-q values, and more importantly, the molecular shapes are now qualitatively different, suggesting decomposition of **1** (Figure 5s, Supporting Information).[62]

SANS data for carbopolyanion **1^{24-}** in THF-d_8 are obtained at room temperature and 170 K (Figure 6s, Supporting Information). However, DAMMIN-based shape reconstructions for **1^{24-}** may not be reliable because of high dependence of the obtained shapes on the applied constraints. Overall, the shapes for **1^{24-}** might be significantly different and of greater size compared to **1** and/or **1^{24-}** forms aggregates. The possibility of aggregation is supported by the observation of highly viscous solutions of **1^{24-}** in THF-d_8 at low temperatures (e.g., 170 K) and apparent increase in R_g with extending the $R_g q$ range of the Guinier law analysis.

Magnetic Shape Anisotropy. The possible shapes for polyradical **1**, which are obtained from conformational searches and SANS-based shape reconstructions, may be viewed as elongated. The simplest approximations for such a shape, for which demagnetizing factors are readily calculated, are ellipsoids of rotation, e.g., a prolate ellipsoid.[63] In such a case, the barrier for coherent rotation of magnetization (E_A) arising from the shape anisotropy is described by eq 2, where ΔN, I_s, and V are the difference of demagnetizing factors between the two longest semiaxes of ellipsoid, magnetization at saturation (per unit volume), and volume of the ellipsoid, respectively.[4,5,27,64a]

$$E_A = (\Delta N I_s^2 V)/2 \qquad (2)$$

Using a prolate ellipsoid (anisometry, $a/b = 2$) of volume and spin density similar to that of **1**, the shape anisotropy barrier

(62) After cleaning of the external windows of the sample cell for **1** at room temperature, the excess of I was still present at 170 K. However, the color of the sample is too dark to see whether the precipitate is present after 4 min at room temperature. After longer times, the color fades and precipitate becomes clearly visible.
(63) (a) Demagnetizing factors for ellipsoids: Osborn, J. A. *Phys. Rev.* **1945**, *67*, 351−357. (b) Stoner, E. C. *Philos. Mag.* **1945**, *36*, 803−821. (c) Inversion of magnetization in single-domain ellipsoids: Stoner, E. C.; Wohlfarth, E. P. *Philos. Trans. R. Soc. London* **1948**, *A240*, 599−642. Reprinted in: *IEEE Trans. Magn.* **1991**, *27*, 3475−3518.
(64) (a) In eq 2, magnetization at saturation is defined by I_s rather than M_{sat} (defined in the preceding sections) according to typical notation. (b) For an ellipsoid with n_{el} ferromagnetically coupled electron spins (total $S = n_{el}/2$) with $I_s = n_{el}\mu_B/V$, E_A in the units temperature (i.e., E_A/k, where k is a Boltzman constant) is as follows: $E_A/k = [(\mu_B^2/k)\Delta N(n_{el}/V)]S$. Thus, for homologous ellipsoids with identical shape ($\Delta N =$ constant) and with identical spin density ($n_{el}/V =$ constant), E_A/k varies linearly with the value of S. (c) For an idealized $4 \times 2 \times 2$ nm prolate ellipsoid ($a/b = 2$) with 24 electron spins, $\Delta N \approx 3.0$ and $n_{el}/V = (9/\pi) \times 10^{21}$ electron cm^{-3}. Thus, for this ellipsoid and homologous ellipsoids, $E_A/k \approx 5S$ mK; for $S = 12$, E_A/k is approximately 60 mK. (d) The $4 \times 3 \times 2$ nm general ellipsoid may possibly be a better approximation to the "dumbbell-like" shape of **1** with dimensions of $4 \times 3 \times 2$ nm. For such ellipsoid, $\Delta N \approx 1.2$ is obtained from demagnetizing factors, leading to E_A/k that is significantly below 60 mK (by a factor of 2−3). (e) One of the reviewers commented on a possible relationship between the anisotropy barriers derived from values of D and those obtained from demagnetizing factors. The discussion will be limited to prolatelike shapes, in which $D < 0$ arises solely from the magnetic dipole−dipole interactions (couplings). For a homologous series of high-spin polyradicals (with similar spin densities and similar shapes), values of $|D|$, scale approximately as $1/S$;[26,40] such polyradicals have approximately constant ESR spectral width, $|D(4S - 2)|$. Therefore, the anisotropy barrier for such polyradicals (or ellipsoids), which is related to the value of $|DS^2|$, varies linearly with the value of S, similarly as determined from demagnetizing factors in ellipsoids.[64b] Furthermore, if the ESR spectral width of 0.006 cm^{-1} (i.e., $4|D/hc|S \approx 0.006$ cm^{-1}) is assumed for **1** with $S = 12$, then the value of $|DS^2|$ is of the order of 30 mK, i.e., similar to that obtained from demagnetizing factors.[40]

for inversion of magnetization of about 60 mK is predicted.[64] This estimate should be viewed as an upper bound.[64] Such a low barrier is consistent with the paramagnetic behavior of **1** at 1.8 K and above. However, for homologous prolate ellipsoids with $a/b \approx 2$ (and same spin density), the shape anisotropy barrier scales as $5S$ mK;[64] i.e., for macromolecules with values of S of the order of several thousands (and spin density similar to that of **1**), the magnetization may become blocked at the readily accessible temperatures of the order of 10 K.

Conclusion

Quantitative magnetic measurements on dendritic-macrocyclic polyradical **1** and its lower homologue **2** confirm the presence of high-spin ground states. The detailed interpretation of the these measurements is complicated by the possible presence of conformations with different exchange couplings, different types of averages for the measured quantities (S, M_{sat}, and χT), and the possibility of incomplete mass transfers. Molecular sizes and shapes for **1** obtained from conformational searches show fair agreement with the shape reconstructions derived from the SANS experiments.

Polyradical **1** with average $S = 10$ may be viewed as a nanometer-sized organic spin cluster, for which estimated shape anisotropy barrier for inversion of magnetization is rather small, in the miliKelvin range. Because the shape anisotropy barriers may scale with S, significant barriers for inversion of magnetization in macromolecules with average $S = 10^3-10^4$ and elongated shapes may be found. The shape anisotropy may in part be responsible for blocking of magnetization in the recently reported organic polymer with average $S \approx 5000$.[1]

Experimental Section

Addition of Small Volumes of Reagents. Reagent volumes of less than 0.3 mL (e.g., of solutions of *t*-BuLi, ZnCl₂, etc.), encountered in micromolar-scale syntheses, were added by counting drops of the reagent solution. Typically, the volumes were calibrated by counting number of drops in 0.4 mL of the reagent solution that was dispensed using 1-mL syringe with a 22-gauge stainless steel needle. Care was taken to mimic the conditions of the actual reaction (rate of addition, position of the needle, temperature, etc.) as closely as possible, using the identical 22-gauge needle.

X-ray Crystallography for 7E. The data were collected on a Bruker SMART system at the University of Minnesota. A colorless, clear crystal (approximate dimensions $0.185 \times 0.105 \times 0.050$ mm³), which was obtained from benzene/methanol solution by slow evaporation, was selected for analysis. Two solvent molecules (benzene) were found from the *E*-map and refined using restraints for the thermal parameter in the bond direction (DELU). Another 1.3 benzene molecules found were heavily disordered in a void and could not be refined to a satisfactory result. An investigation of the void space in the structure, excluding the disordered 1.3 benzene molecules from the refinement, showed that 107 electrons are located in a major void of approximately 640 Å³. (Each benzene molecule occupies 116 Å³ with 42 electrons.) The dataset was corrected for disordered solvent using the program PLATON/ SQUEEZE.[65] The refinement using the corrected data improved the overall structure and the *R*-value by 0.015. However, as the exact amount of solvent is not known, selected values below (and the CIF file deposited on the Web) are incorrect, e.g., formula, formula weight, *F*(000). Crystal data for **7E** were as follows: C₈₄H₈₈Br₄O₄, $M = 1481.18$, triclinic, $a = 16.249(2)$ Å, $b = 16.659(2)$ Å, $c = 16.959(2)$ Å, $\alpha = 90.301(2)°$, $\beta = 108.949(2)°$, $\gamma = 107.420(2)°$, $V = 4115.9(6)$

(65) PLATON: Spek, A. L. *Acta Crystallogr., Sect. A* **1990**, *46*, C34.
(66) Suffert, J. *J. Org. Chem.* **1989**, *54*, 509–510.

Å³, $T = 173(2)$ K, space group $P\bar{1}$, $Z = 2$, Mo Kα ($\lambda = 0.710\,73$ Å). The structure was solved by direct methods and refined by full-matrix least-squares on F^2. A total of 14 492 reflections were observed, and 8206 reflections with $I > 2\sigma(I)$ were recorded. Refinement statistics with 852 parameters was as follows: wR = 0.0847 ($I > 2\sigma(I)$), R = 0.0415 ($I > 2\sigma(I)$), GOF = 0.968.

Tetrabromocalix[4]arene Diols 6. *t*-BuLi (13.20 mL of 1.5 M solution in pentane, 19.80 mmol, 4 equiv) was added to a solution of tetrabromo ether **4** (3.195 g, 4.946 mmol) in THF (500 mL) at −78 °C over the period of about 10 min. After 2−3 h, a solution of diketone **5** (4.000 g, 4.946 mmol) in THF (200 mL) was cannulated to the reaction mixture at −78 °C. The reaction mixture was allowed to warm to ambient temperature for 2 days. Two such reaction mixtures were worked up with water (500 mL) and ether (300 + 200 mL). The combined organic layer was dried over MgSO₄ and then concentrated in vacuo to give the light yellow glassy solid (or light yellow oil). Column chromatography (TLC grade silica gel, 2−10% ether in hexane) gave four fractions (in order of increasing polarity) corresponding to the following isomers: **6A** (2.19 g, 17%), mixture of **6B,C** (1.06 g, 3.5:1, 8%), **6D** (0.604 g, 5%), and **6E** (0.489 g, 4%) as white solids. Small amounts of isomers **6B,C** were further separated (column chromatography or preparative TLC) for spectroscopic characterization. Another set of two reactions on identical scales gave the following results: **6A** (1.778 g, 14%), mixture of **6B,C** (2.312 g, 2.5:1, 18%), **6D** (1.276 g, 10%), and **6E** (0.536 g, 4%). The calculated isotopic intensities for the most intense ions in FABMS of **6A−E** are as follows: C₆₉H₆₉O₃Br₄ at (M − OCH₃)⁺, 1261.2 (15), 1262.2 (11), 1263.2 (61), 1264.2 (45), 1265.2 (100), 1266.2 (69), 1267.2 (80), 1268.2 (48), 1269.2 (30), 1270.2 (15); C₇₀H₇₁O₃Br₄ at (M − OH)⁺, 1275.2 (15), 1276.2 (11), 1277.2 (61), 1278.2 (45), 1279.2 (100), 1280.2 (70), 1281.2 (80), 1282.2 (49), 1283.2 (31), 1284.2 (15), 1285.2 (5).

Diol 6A. The product was softened at 150 °C and melted and became a yellow liquid at 158−160 °C. Anal. Calcd for C₇₀H₇₂O₄Br₄: C, 64.83; H, 5.60. Found: 64.96; H, 4.86. FABMS (3-NBA) cluster *m/z* (% RA for *m/z* = 200−1400): at (M − OCH₃)⁺, 1261.3 (28), 1262.3 (28), 1263.3 (73), 1264.3 (56), 1265.3 (100), 1266.3 (66), 1267.3 (74), 1268.3 (44), 1269.3 (31), 1270.3 (14); at (M − OH)⁺, 1275.4 (24), 1276.4 (20), 1277.4 (66), 1278.4 (55), 1279.3 (100), 1280.4 (68), 1281.4 (77), 1282.4 (46), 1283.3 (32), 1284.3 (18). ¹H NMR (500 MHz, EM = −0.61, GB = 0.47, CDCl₃, ¹H−¹H COSY cross-peaks in aromatic region): 293 K, 7.557 (t, $J = 1.5$, 2 H, 7.399, 6.511), 7.557 (t, $J = 1.5$, 2 H, 7.365, 6.560), 7.399 (s, 2 H, 7.557, 6.511), 7.365 (t, $J = 1$, 2 H, 7.557, 6.560), 7.286 (d, $J = 8$, 4 H, 6.969), 7.248 (d, $J = 8$, 4 H, 6.969), 6.969 (d, $J = 9$, 4 H, 7.286), 6.969 (d, $J = 9$, 4 H, 7.248), 6.560 (s, 2 H, 7.557, 7.365), 6.511 (s, 2 H, 7.557, 7.399), 2.876 (s, 6 H), 2.589 (bs, 2 H, D₂O exch.), 1.326 (s, 18 H), 1.273 (s, 18 H), 1.258 (s, impurity). ¹³C NMR (125 MHz, CDCl₃; 293 K): aromatic region, expected, 20 resonances, found, 20 resonances at 150.8, 150.5, 148.3, 147.7, 146.4, 145.6, 141.9, 137.7, 129.5, 129.4, 129.12, 129.09, 128.7, 127.26, 127.20, 126.8, 125.0, 124.8, 122.4, 122.2; aliphatic region, 86.0, 81.1, 52.0, 34.51, 34.47, 31.30, 31.27, 29.7 (impurity). IR (cm⁻¹): 3565 (O−H), 3458 (O−H), 1567 (Ar), 1084 (C−O−C).

Diol 6B. The product was softened at 152 °C and melted and became a brown liquid at 187−189 °C. FABMS (3-NBA) cluster *m/z* (% RA for *m/z* = 200−1520): at (M − OCH₃)⁺, 1261.1 (26), 1262.2 (24), 1263.2 (73), 1264.2 (56), 1265.2 (100), 1266.2 (71), 1267.2 (73), 1268.2 (48), 1269.2 (27), 1270.2 (13); at (M − OH)⁺, 1275.2 (20), 1276.2 (18), 1277.2 (64), 1278.2 (48), 1279.2 (94), 1280.2 (64), 1281.2 (72), 1282.2 (42), 1283.2 (28), 1284.3 (14). ¹H NMR (500 MHz, EM = −0.59, GB = 0.48, CDCl₃, ¹H−¹H COSY cross-peaks in aromatic region; 293 K): 7.560 (s, 2 H, 7.518, 6.389), 7.518 (s, 2 H, 7.560, 6.389), 7.434 (s, 2 H, 7.270, 6.914), 7.299 (d, $J = 9$, 2 H, 7.036), 7.278 (d, $J = 9$, 4 H, 6.977), 7.278 (d, $J = 9$, 2 H, 6.938), 7.270 (s, 2 H, 7.434, 6.914), 7.036 (d, $J = 8$, 2 H, 7.299), 6.977 (d, $J = 8$, 4 H, 7.278), 6.938 (d, $J = 8$, 2 H, 7.278), 6.914 (s, 2 H, 7.434, 7.270), 6.389 (s, 2 H, 7.560, 7.518), 2.885 (s, 6 H), 2.829 (s, 1 H, exch D₂O),

2.616 (s, 1 H, exch D$_2$O), 1.316 (s, 18 H), 1.304 (s, 9 H), 1.299 (s, 9 H). ^{13}C NMR (125 MHz, CDCl$_3$; 293 K): aromatic region, expected, 24 resonances, found, 24 resonances at 151.0, 150.9, 150.4, 148.2, 148.0, 146.2, 145.4, 141.85, 141.80, 138.0, 130.3, 129.8, 129.3, 129.0, 128.0, 127.6, 127.4, 127.2, 126.8, 125.24, 125.18, 125.13, 122.4, 122.0; aliphatic region, 86.0, 81.4, 81.1, 52.1, 34.52 (br), 34.49, 31.31, 31.29, 31.28. IR (cm^{-1}): 3557 (O–H), 3458 (O–H), 1567 (Ar), 1084 (C–O–C). A small amount of an unknown impurity was present: ^{1}H, 2.270 (s); ^{13}C, 125.5, 30.3.

Diol 6C. The product was changed from white to brown solid at 308 °C and melted and became a brown liquid at 320–322 °C. FABMS (3-NBA) cluster *m/z* (% RA for *m/z* = 200–1520): at (M – OCH$_3$)$^+$. 1260.9 (25), 1261.9 (23), 1262.9 (68), 1263.9 (52), 1264.9 (98), 1265.9 (67), 1266.9 (73), 1267.9 (43), 1268.9 (27), 1269.9 (13); at (M – OH)$^+$, 1274.9 (21), 1275.9 (18), 1276.9 (66), 1277.9 (50), 1278.9 (100), 1279.9 (68), 1280.9 (76), 1281.9 (47), 1282.9 (31), 1283.9 (16). ^{1}H NMR (500 MHz, EM = –1.22, GB = 0.48, CDCl$_3$, ^{1}H–^{1}H COSY cross-peaks in aromatic region; 293 K): 7.517 (t, *J* = 1.5, 4 H, 7.468, 6.488), 7.468 (t, *J* = 1.5, 4 H, 7.517, 6.488), 7.359 (d, *J* = 9, 4 H, 7.033), 7.260 (d, *J* = 9, 4 H, 6.907), 7.033 (d, *J* = 8, 4 H, 7.359), 6.907 (d, *J* = 9, 4 H, 7.260), 6.488 (t, *J* = 1.5, 4 H, 7.517, 7.468), 2.800 (s, 2 H), 2.685 (s, 6 H), 1.318 (s, 18 H), 1.310 (s, 18 H). ^{13}C NMR (125 MHz, CDCl$_3$; 293 K): aromatic region, expected, 14 resonances, found, 14 resonances at 151.1, 150.5, 147.9, 145.7, 142.3, 138.0, 129.9, 128.9, 128.1, 127.50, 127.42, 125.10, 125.02, 122.3; aliphatic region, 85.7, 81.4, 51.8, 34.55, 34.42, 31.31 (EM = –2.88, GB = 0.48), 31.28. IR (cm^{-1}): 3566 (O–H), 3453 (O–H), 1566 (Ar), 1082 (C–O–C). A small amount of an unknown impurity was present: ^{1}H, 2.270 (s); ^{13}C, 125.5, 30.3.

Diol 6D. The product was softened at 187 °C and melted and became a yellow liquid at 223–225 °C. FABMS (3-NBA) cluster *m/z* (% RA for *m/z* = 200–2700): at (M – OCH$_3$)$^+$, 1261.2 (35), 1262.2 (34), 1263.2 (76), 1264.2 (57), 1265.2 (95), 1266.2 (70), 1267.2 (80), 1268.2 (53), 1269.2 (36), 1270.2 (24); at (M – OH)$^+$, 1275.2 (25), 1276.2 (21), 1277.2 (68), 1278.2 (55), 1279.2 (100), 1280.2 (70), 1281.2 (82), 1282.2 (50), 1283.2 (35), 1284.2 (18). ^{1}H NMR (500 MHz, EM = –1.20, GB = 0.80, CDCl$_3$; 293 K): 7.497 (t, *J* = 2, 2 H), 7.478 (t, *J* = 2, 2 H), 7.465 (t, *J* = 2, 4 H), 7.332 (d, *J* = 9, 2 H), 7.320 (d, *J* = 9, 4 H), 7.200 (d, *J* = 9, 2 H), 7.012 (d, *J* = 8, 2 H), 6.974 (d, *J* = 8, 4 H), 6.925 (d, *J* = 9, 2 H), 6.599 (t, *J* = 1.5, 2 H), 6.551 (t, *J* = 1.5, 2 H), 2.865 (s, 3 H), 2.775 (s, 3 H), 2.736 (s, 2 H, D$_2$O exch), 1.328 (s, 9 H), 1.326 (s, 18 H), 1.297 (s, 9 H). ^{13}C{^{1}H} DEPT (135°) NMR (125 MHz, CDCl$_3$; 293 K): aromatic quaternary region, expected, 12 resonances, found, 11 resonances at 151.0 (q), 150.6 (q), 148.0 (q), 147.9 (q), 145.66 (q), 145.61 (q), 142.4 (q), 138.8 (q), 138.2 (q), 122.35 (q), 122.32 (q); aromatic nonquaternary region, expected 12 resonances, found 10 resonances at 130.2, 130.0, 129.4, 128.4, 127.8, 127.36, 127.29, 125.1, 125.0, 124.8; aliphatic region, 86.14 (q), 86.11 (q), 81.3 (q), 52.05, 52.03, 34.55 (q), 34.45 (q), 31.3. IR (cm^{-1}): 3570 (O–H), 3463 (O–H), 1567 (Ar), 1082 (C–O–C).

Diol 6E. The product was yellow solid at 160 °C and melted and became a clear liquid at 197–200 °C. Anal. Calcd for C$_{70}$H$_{72}$O$_4$Br$_4$: C, 64.83; H, 5.60. Found: 65.30; H, 5.94. FABMS (3-NBA) cluster *m/z* (% RA for *m/z* = 280–2400): at (M – OCH$_3$)$^+$, 1261.1 (23), 1262.1 (20), 1263.1 (66), 1264.1 (52), 1265.1 (100), 1266.1 (66), 1267.1 (76), 1268.1 (45), 1269.1 (38), 1270.1 (22); at (M – OH)$^+$, 1275.1 (19), 1276.1 (17), 1277.1 (54), 1278.1 (38), 1279.1 (80), 1280.1 (57), 1281.1 (66), 1282.1 (41), 1283.1 (29), 1284.1 (15). ^{1}H NMR (500 MHz, CDCl$_3$, ^{1}H–^{1}H fast COSY cross-peaks in aromatic region): 293 K, 7.498 (bs, 4 H, 7.360, 6.730), 7.360 (bs, 4 H, 7.498, 6.730), 7.327 (d, *J* = 8, 4 H, 6.960), 7.286 (d, *J* = 8, 4 H, 7.052), 7.052 (d, *J* = 8, 4 H, 7.286), 6.960 (d, *J* = 8, 4 H, 7.327), 6.730 (bs, 4 H, 7.498, 7.360), 2.953 (s, 6 H), 2.669 (s, 2 H, D$_2$O exch), 1.341 (s, 18 H), 1.324 (s, 18 H). ^{13}C{^{1}H} DEPT (135°) NMR (125 MHz, CDCl$_3$; 293 K): aromatic quaternary region, expected, 7 resonances, found, 7 resonances at 150.9 (q), 150.3 (q), 148.1 (q), 145.0 (q), 142.1 (q), 138.7 (q), 122.1 (q); aromatic nonquaternary region, expected, 7 resonances, found 6

resonances at 130.4, 129.7, 127.9, 127.3, 127.2, 125.1; aliphatic region, 86.1 (q), 81.2 (q), 52.1, 34.5 (q), 31.3. ^{1}H NMR (500 MHz, C$_6$D$_6$, ^{1}H–^{1}H fast COSY cross-peaks in aromatic region; 293 K): 7.850 (bs, 4 H, 7.451, 7.150), 7.451 (bs, 4 H, 7.850, 7.150), 7.328 (d, *J* = 8, 4 H, 7.282), 7.282 (d, *J* = 8, 4 H, 7.328), 7.174 (d, *J* = 8, 4 H, 7.039), 7.150 (bs, 4 H, 7.850, 7.451), 7.039 (d, *J* = 8, 4 H, 7.174), 2.821 (s, 6 H), 2.150 (bs, 2 H), 1.341 (s, 18 H), 1.324 (s, 18 H). ^{13}C{^{1}H} DEPT (135°) NMR (125 MHz, C$_6$D$_6$; 293 K): aromatic quaternary region, expected, 7 resonances, found, 6 resonances at 150.9 (q), 149.5 (q), 146.7 (q), 143.3 (q), 139.9 (q), 122.9 (q); aromatic nonquaternary region, expected, 7 resonances, found 7 resonances at 131.1, 130.9, 128.67, 128.3, 128.0, 126.1, 125.7; aliphatic region, 86.9 (q), 81.6 (q), 52.3, 34.9 (q), 34.8(q), 31.72, 31.66. An additional resonance at 128.64 ppm was assigned to C$_6$D$_5$H. IR (cm^{-1}): 3433 (O–H), 1567 (Ar), 1080 (C–O–C).

Tetrabromocalix[4]arene Tetraethers 7. A 100 mL flask with sidearm was charged with NaH (0.300 g of 60% dispersion in mineral oil, 7.722 mmol). After removal of mineral oil with pentane under nitrogen flow, THF (15 mL) was added. The reaction mixture was cooled with an ice bath, and then diol **6A** (1.669 g, 1.287 mmol) in THF (30 mL) was added. The resultant, stirred suspension was allowed to attain ambient temperature over a priod of ∼2 h. Subsequently, iodomethane (1.30 mL, 20.6 mmol) was added at 0 °C. The reaction mixture was allowed to attain ambient temperature overnight. After the usual aqueous workup (ether, MgSO$_4$), the white or light yellow solid was crystallized from ether/MeOH to give pure product **7A** as indicated below. An analogous procedure was used to obtain **7C–E**. The calculated isotopic intensities at (M – OCH$_3$)$^+$ in FABMS of **7A–E** are as follows: C$_{71}$H$_{73}$O$_3$Br$_4$, 1289.2 (14), 1290.2 (11), 1291.2 (61), 1292.2 (46), 1293.2 (100), 1294.2 (70), 1295.2 (80), 1296.2 (49), 1297.2 (31), 1298.2 (15).

Tetraether 7A. From diol **6A** (1.669 g), 1.042 g (62%) of **7A** as white powder was obtained. The product was softened at 305 °C and melted and became a brown liquid at 324–326 °C. Anal. Calcd for C$_{72}$H$_{76}$O$_4$Br$_4$: C, 65.27; H, 5.78. Found: 64.98; H, 5.89. FABMS (3-NBA) cluster *m/z* (% RA for *m/z* = 200–1460): at (M – OCH$_3$)$^+$, 1289.2 (25), 1290.2 (20), 1291.2 (70), 1292.2 (52), 1293.2 (100), 1294.2 (69), 1295.2 (73), 1296.2 (46), 1297.2 (30), 1298.2 (15). ^{1}H NMR (500 MHz, CDCl$_3$, EM = –0.68, GB = 0.46, CDCl$_3$, ^{1}H–^{1}H COSY cross-peaks in aromatic region; 293 K): 7.504, 7.500 (d, *J* = 1.5, d, *J* = 1.5, 8 H, 6.848, 6.434), 7.278 (d, *J* = 9, 8 H, 7.034), 7.034 (d, *J* = 9, 8 H, 7.278), 6.848 (bs, 2 H, 7.504, 7.500), 6.834 (bs, 2 H, 7.504, 7.500), 2.861 (s, 12 H), 1.312 (s, 36 H). (COSY cross-peaks are not resolved for the *J* = 1.5 multiplets.) ^{13}C NMR (125 MHz, CDCl$_3$; 293 K): aromatic region, expected, 12 resonances, found, 12 resonances at 150.4, 146.3, 145.7, 137.8, 130.1, 129.3, 128.9, 128.4, 126.4, 124.8, 121.9, 121.8; aliphatic region, 86.1, 52.2, 34.5, 31.3. IR (cm^{-1}): 1563 (Ar), 1086 (C–O–C).

Tetraether 7C. From 3.5:1 mixture of diols **6B,C** (0.102 g, 0.079 mmol), 0.110 g of yellow viscous solid was obtained. PTLC (10% benzene in hexane) of 0.032 g of the crude mixture gave 0.0268 g (88%) of **7D,C** (3.6:1) as a clear viscous solid.

From 1:8 mixture of diols **6B,C** (20.0 mg, 0.016 mmol), 15.7 mg (74%, single spot in TLC, 3% ether in hexane) of **7D,C** (1:8) as yellow viscous solid was obtained. Treatment with ether/MeOH did not improve the purity of the product.

^{1}H NMR (500 MHz, CDCl$_3$, EM = –1.30, GB = 0.46, ^{1}H–^{1}H COSY cross-peaks in aromatic region; 293 K): 7.466 (d, *J* = 1.5, 8 H, 7.010), 7.322 (d, *J* = 9, 8 H, 7.131), 7.131 (d, *J* = 9, 8 H, 7.322), 7.010 (t, *J* = 1.5, 4 H, 7.466), 2.883 (s, 12 H), 1.323 (s, 36 H). ^{13}C NMR (125 MHz, CDCl$_3$; 293 K): aromatic region, expected, 8 resonances, found, 8 resonances at 150.63, 146.04, 137.9, 129.73, 128.96, 127.2, 124.94, 121.74; aliphatic region, 86.10, 52.15, 34.53, 31.32. IR (cm^{-1}): 1566 (Ar), 1083 (C–O–C).

Tetraether 7D. From diol **6D** (0.348 g, 0.268 mmol), 0.299 g (84%) of **7D** as white powder was obtained. The product was softened at 152

°C, melted at 168−170 °C, and became a clear liquid at 178 °C. From other reactions, 0.573 g (63%) and 0.773 g (83%) of **7D** as white powder after treatment with ether/MeOH were obtained from 0.909 g (0.698 mmol) and 0.914 g (0.705 mmol) of diol **6D**, respectively. The product was softened at 189 °C and melted and became clear liquid at 197−200 °C. Anal. Calcd for $C_{70}H_{72}O_4Br_4$: C, 65.27; H, 5.78. Found: 65.16; H, 5.25. FABMS (3-NBA) cluster m/z (% RA for $m/z = 200-$ 2600): at $(M - OCH_3)^+$, 1289.2 (22), 1290.2 (18), 1291.2 (67), 1292.2 (52), 1293.3 (100), 1294.2 (71), 1295.2 (77), 1296.2 (50), 1297.2 (29), 1298.3 (15). ^{1}H NMR (500 MHz, EM = −1.20, GB = 0.85, CDCl$_3$, ^{1}H−^{1}H FastCOSY cross-peaks in aromatic region; 293 K): 7.522 (t, J = 2, 2H, 7.409, 7.037), 7.502 (t, J = 2, 2 H, 7.409, 6.965), 7.409 (t, J = 2, 2H, 7.522, 7.037), 7.409 (t, J = 2, 2H, 7.502, 6.965), 7.312 (d, J = 9, 4 H, 7.145), 7.312 (d, J = 9, 2 H, 7.010), 7.268 (d, J = 9, 2 H, 7.060), 7.145 (d, J = 8, 4 H, 7.312), 7.060 (d, J = 8, 2 H, 7.268), 7.037 (t, J = 2, 2H, 7.522, 7.409), 7.010 (d, J = 9, 2 H, 7.312), 6.965 (t, J = 2, 2H, 7.502, 7.409), 2.935 (s, 3 H), 2.919 (s, 6 H), 2.895 (s, 3 H), 1.334 (s, 9 H), 1.329 (s, 18 H), 1.314 (s, 9 H). ^{13}C{^{1}H} DEPT (135°) NMR (125 MHz, CDCl$_3$): 293 K, aromatic quaternary region, expected, 12 resonances, found, 12 resonances at 150.53 (q), 150.49 (q), 150.40 (q), 146.3 (q), 146.1 (q), 145.9 (q), 145.8 (q), 138.23 (q), 138.17 (q), 137.7 (q), 121.84 (q), 121.67 (q); aromatic nonquaternary region, expected, 12 resonances, found 12 resonances at 130.3, 129.84, 129.80, 129.5, 128.88, 128.76, 128.35, 127.6, 127.4, 125.04, 124.93 (overlapped with **7C** in mixtures), 124.8; aliphatic region, 86.09 (q), 86.04 (q), 52.4, 52.21, 52.12, 34.53 (q) (overlapped with **7C** in mixtures), 34.51 (q), 31.35. IR (cm^{-1}): 1564 (Ar), 1081 (C−O−C).

Tetraether 7E. From diol **6E** (0.291 g, 0.225 mmol), 0.112 g (38%) of **7E** as white crystals was obtained. Mp: 295−298 °C. Other reactions from diol **6E** (0.345 g, 0.266 mmol; 0.102 g, 0.079 mmol) gave 0.254 g (61%) and 0.058 g (57%), respectively, of **7E** as white solids. The product was softened at 304 °C and melted and became brown liquid at 312−314 °C. Anal. Calcd for $C_{72}H_{76}O_4Br_4$: C, 65.27; H, 5.78. Found: C, 65.29; H, 5.26. FABMS (3-NBA) cluster m/z (% RA for $m/z = 240-2500$): at $(M - OCH_3)^+$, 1289.2 (20), 1290.2 (17), 1291.2 (65), 1292.2 (50), 1293.2 (100), 1294.2 (70), 1295.2 (78), 1296.2 (46), 1297.2 (31), 1298.2 (14). ^{1}H NMR (300 MHz, EM = −1.30, GB = 0.85, CDCl$_3$; 293 K): 7.456 (d, J = 2, 8 H), 7.322 (AB, J = 9, 8 H), 7.147 (t, J = 2, 4 H), 7.119 (AB, J = 9, 8 H), 2.932 (s, 12 H), 1.338 (s, 36 H). ^{1}H NMR (500 MHz, C$_6$D$_6$, ^{1}H−^{1}H COSY cross-peaks in aromatic region; 293 K): 7.699 (d, J = 1.5, 8 H, 7.553), 7.553 (bs, 4 H, 7.699), 7.301 (d, J = 9, 8 H, 7.226), 7.226 (d, J = 9, 8 H, 7.301), 2.783 (s, 12 H), 1.149 (s, 36 H). ^{13}C{^{1}H} DEPT (135°) NMR (125 MHz, C$_6$D$_6$; 293 K): aromatic quaternary region, expected, 4 resonances, found, 4 resonances at 150.8 (q), 146.7 (q), 140.2 (q), 122.5 (q); aromatic nonquaternary region, expected, 4 resonances, found 4 resonances at 131.6, 129.3, 128.4, 126.2; aliphatic region, 86.9 (q), 52.3, 34.8 (q), 31.7. IR (cm^{-1}): 1565 (Ar), 1083 (C−O−C).

24-Ether 1-(OMe)$_{24}$. t-BuLi (0.136 mL of 1.855 M solution in pentane,[66] 0.253 mmol) was added to bromopentaether **8** (0.186 g, 0.117 mmol) in THF (1.3 mL) in a heavy-wall Schlenk vessel at −78 °C. After 2 h at −78 °C, the reaction mixture was allowed to attain −20 °C for 10 min and then recooled to −78 °C. Following the addition of ZnCl$_2$ (0.13 mL of 1.03 M solution in ether, 0.134 mmol), the reaction mixture was allowed to attain ambient temperature. In a Vacuum Atmospheres glovebox, Pd(PPh$_3$)$_4$ (5.0 mg, 4.3 μmol) and tetrabromocalix[4]arene tetraether **7E** (25.9 mg, 19.5 μmol) were added to the reaction mixture. Subsequently, the reaction mixture was stirred at 100 °C for 3 days. Following the usual aqueous workup, two consecutive purifications by column chromatography (4−8% ether in hexane) and treatments with MeOH/ether gave 24-ether **1-(OMe)$_{24}$** as a white powder (54.7 mg, 40%). Three additional reactions, each starting from 0.2−0.400 g of bromopentaether **8**, gave 24-ether in 28, 13, and 16% yields.

The following side products were isolated by column chromatography and treated with ether/MeOH to give white powders: dendrimer

quenching product **8-H** (40.7 mg, 23%); homocoupling product **10** (24.7 mg, 7%); tricoupling product **12** (1.8 mg, 1%). Another isolation of **10**, without treatment with ether/MeOH, gave 16.4 mg (9%) of clear oil.

24-Ether 1-(OMe)$_{24}$: softening at 186 °C and melting at 200−201 °C (clear liquid). Anal. Calcd for $C_{504}H_{592}O_{24}$: C, 86.06; H, 8.48. Found: 86.60; H, 8.22. FABMS (3-NBA) cluster m/z (% RA for $m/z = 3200-7400$): at $(M - OCH_3)^+$, 6998.5 (35), 6999.5 (52), 7000.5 (74), 7001.5 (90), 7002.5 (100), 7003.5 (75), 7004.5 (71), 7005.5 (49), 7006.5 (31); calcd for $C_{503}H_{589}O_{23}$ at $(M - OCH_3)^+$, 6998.5 (11), 6999.5 (32), 7000.5 (61), 7001.5 (88), 7002.5 (100), 7003.5 (96), 7004.5 (78), 7005.5 (56), 7006.5 (35). ^{1}H NMR (500 MHz) spectra for **1-(OMe)$_{24}$** were obtained in C$_6$D$_6$ (293−348 K), toluene-d_8 (293−383 K), and tetrachloroethylene (293−383 K). The best resolved spectra were obtained in benzene-d_6, and only those are listed below. ^{1}H NMR (500 MHz, C$_6$D$_6$): 293 K, 8.10−7.00 (br m, 196 H), 3.264 (s, 12 H), 2.947 (s, 48 H), 2.869 (s, 12 H), 1.211 (s, 144 H), 1.205 (s, 144 H), 1.062 (s, 36 H); 328 K, 8.10−7.00 (br m, 196 H), 3.265 (s, 12 H), 2.949 (s, 48 H), 2.885 (s, 12 H), 1.214 (s, 288 H), 1.086 (s, 36 H). ^{1}H NMR (500 MHz, EM = −1.20, GB = 0.90, benzene-d_6, ^{1}H−^{1}H COSY cross-peaks in aromatic region; 348 K): 7.97 (br, 4 H), 7.90 (br, 8 H), 7.817 (d, J = 2, 16 H, 7.673), 7.673 (t, J = 2, 8 H, 7.817), 7.636 (d, J = 9, 8 H, 7.260), 7.455 (d, J = 9, 32 H, 7.227), 7.448 (d, J = 8, 32 H, 7.219), 7.423 (d, J = 8, 8 H, 7.352), 7.352 (d, J = 8, 8 H, 7.423), 7.260 (d, J = 9, 8 H, 7.636), 7.227 (d, J = 9, 32 H, 7.455), 7.219 (d, J = 9, 32 H, 7.448), 3.262 (s, 12 H), 2.952 (s, 48 H), 2.896 (s, 12 H), 1.220 (s, 288 H), 1.106 (s, 36 H). ^{13}C{^{1}H} DEPT (135°) NMR (125 MHz, EM = −0.90 Hz, GB = 1.90 Hz, C$_6$D$_6$, ^{1}H−^{13}C HMQC-GS cross-peaks in aromatic nonquaternary region; 348 K): aromatic quaternary region, expected, 10 resonances, found, 9 resonances at 150.3 (q), 150.0 (q), 145.02 (q), 144.98 (q), 143.8 (q), 143.2 (q), 142.8 (q), 140.6 (q), 140.5 (q); aromatic nonquaternary region, expected, 10 resonances, found 9 resonances at 131.2 (7.352), 130.0 (7.673), 129.6 (7.455, 7.448), 128.8 (7.636), 127.9 (7.817), 127.5 (br, 7.90), 127.0 (7.423), 125.7 (7.260), 125.1 (7.227, 7.219); aliphatic region, 88.5 (q), 88.1 (q), 87.9 (q), 52.90, 52.87, 52.6, 34.9 (q), 31.99, 31.96 (EM = −0.9, GB = 1.0). Note: the ^{13}C resonance at 125.1 ppm corresponds to two resonances at 125.15 and 125.13 (EM = −0.77 and GB = 0.40) at 293 K. IR (cm^{-1}): 1595 (ArH), 1082 (C−O−C). GPC/MALS: Table 4s, Supporting Information.

Octaether 2-(OMe)$_8$. A procedure analogous to that for **1-(OMe)$_{24}$** was used. t-BuLi (0.189 mL of 1.855 M solution in pentane,[66] 0.351 mmol) was added to bromoether **9** (76.7 mg, 0.165 mmol) in THF (1.5 mL) in a heavy-wall Schlenk vessel at −78 °C. After 2 h at −78 °C, the reaction mixture was warmed to −20 °C for 10 min and then recooled to −78 °C. Following addition of ZnCl$_2$ (0.17 mL of 1.03 M solution in ether, 0.175 mmol), the reaction mixture was allowed to attain ambient temperature. In a Vacuum Atmospheres glovebox, Pd(PPh$_3$)$_4$ (6.0 mg, 5.2 μmol) and tetrabromocalix[4]arene tetraether **7E** (36.5 mg, 27.5 μmol) were added to the reaction mixture. Subsequently, the reaction mixture was heated at 100 °C for 3 days. Following the usual workup, column chromatography (preheated silica at 200 °C overnight, 3−5% ether in hexane) and treatment with ether/ MeOH, 8.7 mg (12%) of **2-(OMe)$_8$** as a white powder was obtained. (The purity of fractions corresponding to **2-(OMe)$_8$** was checked with ^{1}H NMR before combining and filtering through the cotton plug.) Similarly, 6.6 mg (10%) of homocoupling side product **11** was obtained as a white powder.

A second reaction yielded 23.6 mg (16%) of **2-(OMe)$_8$** as a white powder; it was performed on a double scale using t-BuLi (0.45 mL of 1.5 M solution in pentane, 0.675 mmol), bromoether **9** (150 mg, 0.322 mmol) in THF (3.0 mL), and tetraether **7E** (75.0 mg, 56.7 μmol).

A third reaction yielded 21.7 mg (16%) of **2-(OMe)$_8$** as a white powder; it was carried out using t-BuLi (0.45 mL of 1.5 M solution in pentane, 0.675 mmol), bromoether **9** (150 mg, 0.322 mmol) in THF (3.0 mL), and tetraether **7E** (70.1 mg, 52.9 μmol).
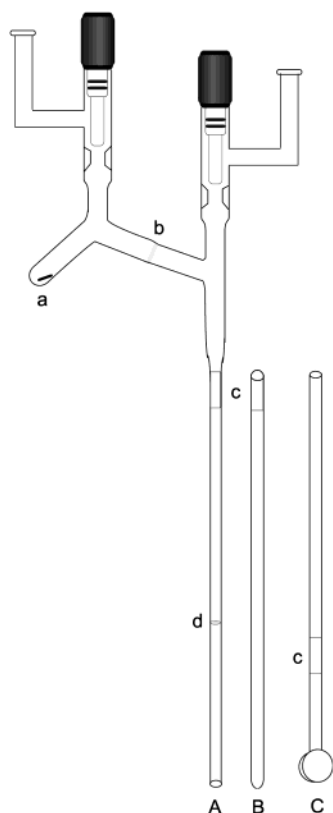
Figure 13. Vessel for preparation of polyanions and polyradicals for SQUID magnetometry (tube A), ESR spectroscopy (tube B), SANS (cylindrical cell C), and NMR spectroscopy (sample tube not shown): (a) sample compartment with Teflon-coated magnetic stirbar; (b) glass frit (course); (c) Pyrex-to-quartz seal; (d) thin bottom (~6 cm from the end of the tube). Solv-seal joints and Kontes (or Chemglass) vacuum stopcocks are used.

Octaether 2-(OMe)$_8$: softening at 201 °C and melting at 226–229 °C. Anal. Calcd for $C_{184}H_{208}O_8$: C, 86.75; H, 8.23. Found: 85.39; H, 7.99. FABMS (3-NBA) cluster *m/z* (% RA for *m/z* = 700–4300): at (M − OCH$_3$)$^+$, 2514.6 (65), 2515.6 (100), 2516.6 (95), 2517.6 (65), 2518.5 (40); calcd for $C_{183}H_{205}O_7$, 2514.6 (45), 2515.6 (95), 2516.6 (100), 2517.6 (70), 2518.6 (35). ^{1}H NMR (500 MHz, C$_6$D$_6$, ^{1}H–^{1}H COSY cross-peaks in aromatic region; 293 K): 8.06 (br, 4 H, 7.95), 7.95 (br, 8 H, 8.06), 7.627 (d, *J* = 8, 8 H, 7.218), 7.533 (d, *J* = 8, 16 H, 7.265), 7.472 (d, *J* = 8, 8 H, 7.439), 7.439 (d, *J* = 8, 8 H, 7.472), 7.265 (d, *J* = 8, 16 H, 7.533), 7.218 (d, *J* = 8, 8 H, 7.627), 3.132 (s, 12 H), 3.035 (s, 12 H), 1.211 (s, 72 H), 1.060 (s, 36 H). ^{13}C{^{1}H} DEPT (135°) NMR (125 MHz, C$_6$D$_6$, ^{1}H–^{13}C HSQC-GS cross-peaks in aromatic nonquaternary region; 293 K): aromatic quaternary region, expected, 8 resonances, found, 7 resonances at 150.1 (q), 150.0 (q), 145.3 (q), 144.3 (q), 142.3 (q), 140.54 (q), 140.47 (q); aromatic nonquaternary region, expected, 8 resonances, found 8 resonances at 130.4 (8.06, br), 130.1 (7.472), 129.5 (7.533), 128.8 (7.627), 127.5 (7.95), 127.3 (7.439), 125.8 (7.218), 125.3 (7.265); aliphatic region, 88.0 (q), 52.6, 52.4, 34.78 (q), 34.72 (q), 31.8. IR (cm^{-1}): 1595 (ArH), 1081 (C−O−C). GPC/MALS: Table 4s, Supporting Information.

Carbopolyanion 1^{24-} for NMR or SANS Studies. Polyether 1-(OMe)$_{24}$ (11.40 mg, 1.62 μmol) was placed in a glass reaction vessel, equipped with a 5-mm NMR sample tube or a quartz cylindrical cell (Figure 13). Carbopolyanion was generated by following the procedure for polyradical 1, which is described in the following paragraph. After the solution of carbopolyanion was filtered into the NMR tube or SANS cell, the sample vessel was flame sealed and stored in liquid nitrogen for subsequent studies. ^{1}H NMR (500 MHz, THF-d_8): 293 K, 7.40–6.10 (m, 196 H), 1.164 (s, 320 H); 193 K, 7.8–5.3 (bm), 1.4–0.9 (bm),

both resonances for THF-d_7 remain relatively sharp. ^{13}C NMR (125 MHz, pulse delay = 0.1 s, acquisition time = 0.5 s, 7 × 10^4 scans, THF-d_8; 293 K): aromatic region, expected, 24 resonances, found, 10 resonances at 152.4, 149.2, 145.6, 144.3, 132.3, 125.6, 120.9, 120.3, 119.3, 118.2; aliphatic region, 85.8 (Ar$_3$C), 34.2, 32.6, 32.4 (30.7, imp).

Polyradicals 1 and 2. Samples for Magnetic Measurements. 24-Ether 1-(OMe)$_{24}$ (0.50–1.60 mg, 70–230 nmol) was placed in a glass reaction vessel, equipped with coarse glass frit, two high-vacuum PTFE stopcocks, and a 5-mm o.d. quartz tube with thin bottom 6 cm from the end of the tube (Figure 13). The vessel containing polyether was heated overnight under vacuum; i.e., part of the vessel containing polyether was immersed in an oil bath at 60 °C and the rest of the vessel was heated at 200 °C using heating tape. Subsequently, the vessel was transferred to a glovebox and a small drop of Na/K alloy was added. Following attachment of the vessel to vacuum line, Na/K was allowed to come in contact with polyether, and THF-d_8 (0.06–0.08 mL, 99.95% D) was immediately vacuum-transferred from sodium/benzophenone. After 3–5 days of stirring at 10 °C, the reaction mixture was filtered under temperature gradient into the quartz tube. (An alternative procedure was based upon preparation of carbopolyanion in a glovebox equipped with oven/antechamber.) Iodine (99.999%, ultradry) was vacuum-transferred in small portions to the reaction mixture at −103 to −106 °C, until the final yellow-brown color of 1 appeared. The tube was flame sealed (total length of about 20 cm) and stored in liquid nitrogen prior to insertion to SQUID magnetometer. Analogous procedures were used for octaradical 2 and tetraradical 3. The dilute sample of 2 was prepared using a previously reported method, in which the measured amount of polyradical is not known.[21]

Samples for SANS Measurements. The procedure was based upon 10–30 mg of 24-ether 1-(OMe)$_{24}$; quartz cylindrical cells with 2-mm and 5-mm optical paths were used (Figure 13).

Approximately twice the volume of THF-d_8, compared to the samples for magnetic measurements, was used for generation of carbopolyanion. For polyradical generation, iodine and THF-d_8 were vacuum transferred in small portions until the desired color and volume in the cell were attained. Subsequently, the cells were flame sealed; the quartz seal, above the cylindrical part of the cell, had to be <2 cm long to provide an adequate fit to the SANS sample holder.

Quenching Studies. 1-H$_{24}$. A cylindrical SANS cell, containing 1^{24-} (prepared from 29.56 mg, 4.20 μmol, of 1-(OMe)$_{24}$) in THF-d_8, was immersed under argon-bubbled MeOH (100 mL) at room temperature. The cell was cracked, and the brown mixture was leaking out to be in contact with MeOH to form a white precipitate. Following the usual aqueous workup with hexane, PTLC (25% chloroform in hexane), and treatment with ether/MeOH, 10.9 mg (41%) of the less polar (F1) and 2.6 mg (10%) of the more polar (F2) fractions of 1-H$_{24}$ were obtained as white powders. Although the R_f values for F1 and F2 are significantly different on silica, their ^{1}H NMR spectra are almost identical.

F1: softening at 194 °C and melting at 204–206 °C (clear liquid). ^{1}H NMR (500 MHz, CDCl$_3$; 293 K): 7.25–6.65 (m, 196 H), 5.45–5.35 (m, 4 H), 5.219, 5.178 (s, s, 19 H), 1.35–1.05 (m, 325 H). ^{13}C NMR (125 MHz, CDCl$_3$; 293 K): aromatic region, expected 20 resonances, found 18 resonances at 148.5, 144.5 (br), 143.7 (br), 142.5, 141.34, 141.26, 140.5 (br), 138.4, 129.5, 128.86, 128.83, 128.6, 128.4, 126.6, 126.2 (br), 125.5, 125.3–124.8 (br), 124.9; aliphatic region, 56.7 (br), 56.4 (br), 55.9, 34.3, 31.1. IR (cm^{-1}): 1595 (ArH). GPC/MALS: Table 4s, Supporting Information. SANS (THF-d_8): see main text.

F2: softening at 190 °C and melting at 204–206 °C (yellow liquid). ^{1}H NMR (500 MHz, CDCl$_3$; 293 K): 7.23–6.60 (m, 196 H), 5.45–5.35 (m, 4 H), 5.217, 5.178 (s, s, 18 H), 1.37–1.00 (m, 317 H). IR (cm^{-1}): 1595 (ArH).

2-H$_8$. A small portion of polyradical 2 in THF (prepared from 9.4 mg of octaether 1-(OMe)$_8$) was transferred to a quartz tube for magnetic measurements, and the remaining polyradical was stirred with Na/K at −95 to −78 °C for several hours and then quenched with MeOH. The usual aqueous workup, followed by PTLC (2.5% ether in hexane), gave

2-H$_8$ as glassy solid (6.1 mg, 70%) with softening at 190 °C and melting at 202−205 °C (yellow liquid). FABMS (3-NBA) cluster m/z (% RA for m/z = 2288−2333, S/N ≈ 2.5/1): 2305.5 (65), 2306.5 (85), 2307.5 (95), 2308.5 (100), 2309.5 (85), 2310.5 (65); calcd for C$_{176}$H$_{193}$ (M + H)$^+$, 2306.5 (50), 2307.5 (100), 2308.5 (98), 2309.5 (65), 2310.5 (30). ^{1}H NMR (500 MHz, CDCl$_3$; 293 K): 7.5−6.7 (m, 60 H), 5.8−4.4 (8 H), 1.35−1.1 (m, 107 H). IR (cm^{-1}): 1594 (ArH).

SQUID Magnetometry. A Quantum Design (San Diego, CA) MPMS5S (with continuous temperature control) was used. The sample tubes were inserted to the magnetometer at low temperature under helium atmosphere and then evacuated and purged with helium, as described elsewhere. Following the measurements, sample tubes were stored at ambient temperature for several weeks, until they were diamagnetic in the 1.8−150 K range. Such samples were carefully reinserted to the magnetometer, with the sample chamber at 200 or 290 K. Then the temperature was slowly lowered to 10 K to condense the solvent and to freeze the sample. The identical sequence of measurements, as for the original sample, was carried out. The resultant data were used for the point-by-point correction for diamagnetism.

Numerical Curve Fitting for Magnetic Data. The SigmaPlot for Windows software package was used for numerical curve fitting. The reliability of a fit is measured by the parameter dependence, which is defined as follows: *dependence = 1 − ((variance of the parameter, other parameters constant)/(variance of the parameter, other parameters changing))*. Values close to 1 indicate overparametrized fit.

Up to four variable parameters, J/k (spin coupling constant in Kelvins), N (number of moles of polyradical), Θ (mean field parameter for small intermolecular magnetic interactions), and M_{dia} (correction for diamagnetism), are used for fitting MT vs T data over wide range of T. In **1**, Θ does not affect the fits and it is omitted ($\Theta = 0$), as the intermolecular magnetic interactions are essentially negligible. With the exception of one sample of **1**, in which M_{dia} was more than 1% of the total diamagnetism after point-by-point correction, $M_{dia} = 0$ was set. Thus, no more than three variable parameters were used. Equations for magnetization, $M(T,H)$, are obtained using the standard statistical mechanical procedures for energy eigenvalues, derived from Heisenberg Hamiltonian.[26,46−48]

M vs H data at low temperatures ($T = 1.8, 3, 5, 10$ K) were analyzed with Brillouin functions as described in the text.

For **1**, an alternative procedure for analysis of the M vs H data involved fitting of the M vs H/T data to linear combinations of Brillouin functions (B(S_i)) weighed with fractions (x_i) of spin systems with spin S_i. Two different percolation models were used to obtain values of x_i and S_i.

The first percolation model, which was employed in the preliminary communication,[22] used eq 3.

$$M/M_{sat} = \Sigma_i B(S_i)x_i/\Sigma_i x_i \tag{3}$$

The model assumed ferromagnetic coupling between all nearest neighbor arylmethyls. Two variable parameters, p and M_{sat}, were used. Parameter p was the probability that triarylmethyl site had an intact radical. Because the value of M_{sat} was a variable parameter, this model was not quantitative. Enumeration of configurations with 0−4 defects

at the four 4-biphenyl-substituted sites gave the following values of x_i and S_i: $x_i = p^4$, $4p^3(1 − p)$, $6p^2(1 − p)^2$, $4p(1 − p)^3$, $(1 − p)^4$, and $8[p^3(1 − p) + 3p^2(1 − p)^2 + 3p(1 − p)^3 + (1 − p)^4]$ and $S_i = 2 + 10p$, $1.5 + 8p$, $1 + 6p$, $0.5 + 4p$, $2p$, and p, where $i = 1, 2, ... 6$. Because in eq 2 the Brillouin functions were not explicitly multiplied by values of spin, S_i, fractions x_i included S_i. Therefore, spin-average spin S_s should be defined as shown in eq 4.[51]

$$S_s = \Sigma_i S_i x_i/\Sigma_i x_i \tag{4}$$

For polyradical **1**, eq 4 could be simplified: $S_s = 12p/(9 − 8p)$.

The second percolation model, used in this work, was based on eq 5:

$$M = 11180N\Sigma_i A_i B(S_i) \tag{5}$$

Coefficients A_i and spin values S_i are optimized through two variable parameters, q and p. Parameter p was defined as in the first percolation model. Parameter q was the probability that a biphenylene moiety mediates ferromagnetic (vs antiferromagnetic) coupling. This model was quantitative, using number of moles (N) of polyradical (or polyether) as an input; M_{sat} was not a variable parameter. Configurations with 0−4 defects at the four 4-biphenyl-substituted sites and 0−4 antiferromagnetic couplings across four biphenylene coupling units were enumerated, leading to 1280 spin systems; however, only 10 spin values (S_i, $i = 0−9$) were unique. Elucidation of all values of S_i and coefficients A_i for 24-radical **1** followed general methods as reported elsewhere.[28a]

Supporting Information Available: An experimental section (materials and special procedures, NMR spectroscopy and other analyses, characterization data for **8-H**, **8-D**, **10**, **11**, and **12-(OMe)$_{19}$**, SANS instrumental setup and sample handling, numerical curve fitting for the SANS data), Tables 1s−4s (summary of NMR data for **6** and **7**, summary of GPC/MALS data), Figures 1s−6s (FAB MS for **2-(OMe)$_8$** and **12-(OMe)$_{19}$**, summary plot of GPC/MALS data, selected NMR spectra for **2-(OMe)$_8$**, SANS plots for polyradical **1** and polyanion **1$^{24−}$**), and an X-ray crystallographic file for **7E** in CIF format. This material is available free of charge via the Internet at http://pubs.acs.org.

JA031548J